

Permutation invariant matrix quantum thermodynamics and negative specific heat capacities in large N systems.

Denjoe O'Connor^{a,*}, Sanjaye Ramgoolam^{a,b,c,†}

^a*School of Theoretical Physics*

Dublin Institute of Theoretical Physics, 10 Burlington Road, Dublin 4, Ireland

^b*School of Physics and Astronomy, Centre for Research in String Theory
Queen Mary University of London, London E1 4NS, United Kingdom*

^c*School of Physics and Mandelstam Institute for Theoretical Physics,
University of Witwatersrand, Wits, 2050, South Africa*

E-mails: *denjoe@stp.dias.ie, †s.ramgoolam@qmul.ac.uk

Abstract

We study the thermodynamic properties of the simplest gauged permutation invariant matrix quantum mechanical system of oscillators, for general matrix size N . In the canonical ensemble, the model has a transition at a temperature T given by $x = e^{-1/T} \sim x_c = e^{-1/T_c} = \frac{\log N}{N}$, characterised by a sharp peak in the specific heat capacity (SHC), which separates a high temperature from a low temperature region. The peak grows and the low-temperature region shrinks to zero with increasing N . In the micro-canonical ensemble, for finite N , there is a low energy phase with negative SHC and a high energy phase with positive SHC. The low-energy phase is dominated by a super-exponential growth of degeneracies as a function of energy which is directly related to the rapid growth in the number of directed graphs, with any number of vertices, as a function of the number of edges. The two ensembles have matching behaviour above the transition temperature. We further provide evidence that these thermodynamic properties hold in systems with $U(N)$ symmetry such as the zero charge sector of the 2-matrix model and in certain tensor models. We discuss the implications of these observations for the negative specific heat capacities in gravity using the AdS/CFT correspondence.

Contents

1	Introduction	3
2	Bosonic GPIMQM Partition functions : Review	9
3	GPIMQ-thermodynamics in the canonical ensemble : finite N cross-over transition and vanishing Hagedorn temperature	11
3.1	Super-exponential degeneracies and vanishing Hagedorn temperature . . .	12
3.2	Thermodynamic quantities in the canonical ensemble	13
3.2.1	Energy versus temperature	15
3.2.2	Specific heat capacity versus temperature	15
3.2.3	Entropy versus temperature and Entropy as a function of Energy	19
3.3	High temperature limit and N^2 simple harmonic oscillator thermodynamics	21
3.4	Zeroes in the complex plane	21
4	PIMQ-Thermodynamics in the micro-canonical ensemble : Negative specific heat and (in)equivalence of ensembles	23
4.1	Micro-canonical ensemble and negative specific heat capacities	23
4.2	Thermodynamic quantities in the micro-canonical ensemble	24
4.2.1	Energy versus micro-canonical temperature	25
4.2.2	Specific heat capacity versus micro-canonical temperature	27
4.3	Equivalence and in-equivalence of ensembles	28
5	High temperature expansion of PIMQ-Thermo and small cycle dominance	29
5.1	Cycle structures and the high temperature expansion	31
5.2	Breakdown of the high T expansion and the characteristic scale $x_c = \frac{\log N}{N}$.	35
6	Path Integral for Tensor Models	36
6.1	Complex-Vectors	39
6.2	Two-Tensors	40
6.3	Three-Tensors	41
6.4	Hermitian Matrices with adjoint $U(N)$ action.	42
6.5	The Adjoint Matrix system with $d = 2$ and the $U(1)$ -Charge-0 Sector . . .	43
7	High Temperature Limits from path integrals	44
7.1	Matrix Models under Adjoint Action of $U(N)$	45
7.2	Tensor Models	46
7.2.1	Counting Complex Vector Invariants	47

8	Hagedorn transitions in $U(N)$ invariant models and negative SHC in tensor models	47
8.1	3-index complex tensor model : Phase structure and computational evidence.	50
9	Negative SHCs in matrix quantum mechanical models and AdS/CFT	52
9.1	Super-exponential and sub-exponential growths of combinatorial sequences and negative specific heat capacities	53
9.2	Negative SHCs from zero-charge sector of complex matrix quantum mechanics and AdS/CFT	55
9.3	Negative SHC with super-exponential growth of degeneracies in multi-matrix models	57
10	Summary and Outlook	60
A	Multi-harmonic oscillator and ensemble equivalence	62
B	Proving that the first sub-leading term in the high temperature expansion is from $p = [2, 1^{N-2}]$	65
C	Integer sequences, Hagedorn and heat capacity	68
D	SAGE computation for zero charge sector of 2-matrix models	70
E	SAGE computation for negative SHC in multi-matrix model with $d = n$ scaling	70

1 Introduction

Matrix quantum mechanics (MQM) models with $U(N)$ gauge symmetry groups provide avenues to inform the solution of questions in quantum gravity through gauge-gravity dualities [1, 2, 3, 4, 5]. In this paper we demonstrate that simple non-interacting matrix models, where S_N replaces $U(N)$ gauge symmetry, provide a setting where negative specific heat capacities and associated in-equivalence of thermodynamic ensembles emerge naturally. These features are of interest in connection with gravitational thermodynamics in holographic quantum mechanical systems. This work relies on analytic and computational development of the results in [6, 7].

An important strand of research in gauge-gravity duality investigates the relation between the gravitational thermodynamics in AdS and the CFT thermodynamics. The transition in semi-classical gravity between the vacuum AdS solution and the AdS black hole geometry was shown to imply a phase transition at large 't Hooft coupling in the

large N limit of $N = 4$ SYM theory [4]. Motivated by a study of phase structures in weakly coupled gauge theories, it was shown in [8] that the $U(N)$ invariant sector of the 2-matrix harmonic oscillator has an exponential growth of the degeneracies at low energy levels and a finite Hagedorn temperature in the large N limit. This mirrors properties of weakly coupled gauge theories [9] in the large N limit. Finite N partition functions for 2-matrix quantum mechanics were analysed for N up to 7 [10] and the Hagedorn transition related to a convergence of zeroes to a point on the real axis $x = e^{-1/T} = e^{-\beta}$. Recent work has shown that super-symmetric matrix models with known gravity duals can have non-supersymmetric analogs which capture similar large N thermodynamics [11, 12].

MQM models also play a role in earlier examples of gauge-string duality such as large N two-dimensional Yang-Mills theories [14] where the unitary matrix models [15] were understood to capture the state space and amplitudes. Particular sectors of the AdS/CFT correspondence are also controlled by MQM models, e.g. the half-BPS sector by one-matrix models [16, 17, 18] and less super-symmetric sectors by multi-matrix models [19, 20]. Permutation groups arise as hidden symmetries, i.e. groups which are not manifest symmetries of the action, but which control the combinatorics of many problems in gauge-string duality through the mathematics of Schur-Weyl duality, as explained in the reviews [21, 22]. Permutation groups also arise as more manifest symmetries in the AdS/CFT correspondence, notably in the case of AdS3/CFT2 [3] where the CFT is an orbifold by S_N .

In addition to their role as time-dependent variables in quantum mechanical systems, matrices also arise as integration variables in zero-dimensional matrix models. An example, related to the BFSS model, is the zero-dimensional IKKT model [23]. Simple matrix models also have a long history of applications in modelling statistical characteristics of physical data ranging from nuclear energy levels to financial correlation matrices [24, 25, 26]. The standard matrix models widely studied in the context of holography or of matrix statistics have continuous manifest symmetries such as $U(N)$.

The study of permutation groups as manifest, as opposed to hidden, symmetries in matrix models has been initiated in the context of applications of matrix models to ensembles of matrices in computational linguistics [27]. The general 13-parameter Gaussian model [28] has been shown to describe approximate gaussianity in matrix representations of words [29, 30] and a reduction to a 4-parameter model appropriate for symmetric traceless matrices has been used to demonstrate approximate gaussianity for statistical correlation matrices [31].

While there is not yet a gauge-string duality conjecture relating these matrix models to appropriate gravitational or stringy duals, it is important to investigate whether the large N characteristics of these matrix models bear significant similarities to those of matrix models which do have such known duals. With these motivations, a large N factorisation property for matrix model correlators, and for matrix quantum mechanics inner products,

was established using properties of partition algebras which arise as hidden symmetries through the mechanisms of Schur-Weyl duality [32, 33]. An important aspect of the permutation invariant matrix observables is their relation to the counting of directed graphs, which was observed in [27, 28], then studied in detail and generalised to multi-matrix permutation invariants in [34]. The relevant number sequence for the case of 1-matrix invariants is [35].

In [6] we gave, following earlier work in the context of the BFSS model [13], the path integral formulation for the partition function of permutation invariant matrix models, by discretising the Euclidean time direction so that parallel transport is implemented by group elements as in lattice gauge theory, and taking a continuum limit. This allowed us to recover the Molien-Weyl formula in the Gaussian case. In [7] we derived explicit formulae for the partition functions of the general 11-parameter Gaussian permutation invariant harmonic oscillator quantum mechanical systems.

The different thermodynamic characteristics of single-matrix, multi-matrix and tensor models at large N are largely due to properties of associated combinatorial integer sequences. An important feature of the counting of permutation invariants of a single matrix is the very rapid growth of the dimension of the space of invariants as a function of degree k for $k \leq N/2$. We will refer to the counting in this regime as the stable large N regime. This growth is related to a counting of directed graphs with k edges and any number of vertices. It is super-exponential as we will discuss in more detail in section 3 of this paper.

A similar very rapid growth of invariants occurs in tensor models with invariance under $U(N)$ or other continuous symmetry groups. The 3-index complex tensor model with $U(N) \times U(N) \times U(N)$ gauge symmetry, which has been studied with motivations from quantum gravity [36, 37] is a case where the large N stable counting is related to the counting of bi-partite ribbon graphs [38] [40]. Super-exponential growth in degeneracies in the stable regime have been recognised to lead to a vanishing Hagedorn temperature in the large N limit [41][42]. An open question has been to clarify the physics of these zero-temperature Hagedorn transitions in the context of matrix and tensor models at large N . This paper addresses the question.

We summarise the principal results of this paper, starting with results pertaining to the simplest gauged permutation invariant quantum matrix (GPIQM) model

- Using the exact finite N formula (2.15) for the canonical partition function from [7], we derive the all-orders high temperature expansion organised in terms of the degrees of singularities of the partition function at $x = 1$. The formula for the degrees (5.5) is a function of partitions p of N .
- We prove, using the equation (5.5), that the leading term in the high temperature expansion comes from $p = [1^N]$. The high-temperature limit is also derived from a

path integral point of view.

- We prove, using equation (5.5), that the second term in the high temperature expansion comes from $p = [2, 1^{N-1}]$. By comparing the first and second terms, we obtain an all orders large N formula for the breakdown scale x_{bkdn} of the high temperature expansion. The first term in this large N formula identifies a characteristic scale $x_c = \frac{\log N}{N}$.
- In the canonical ensemble, there is a Hagedorn-like cross-over transition at a temperature which approaches zero in the large N limit. The transition is associated with a rapid increase in the expectation value of the energy as the temperature is increased through the transition. This is signalled by a peak in the specific heat capacity located at $x_{\text{max}} \sim x_c = \frac{\log N}{N}$. The zero temperature limit is evidenced in Figure 17.
- The microcanonical and canonical ensembles are only equivalent above the transition temperature. This is illustrated in Figure 15.
- In the microcanonical ensemble the GPIQM exhibits negative heat capacity at energies below the transition and for asymptotically large N the specific heat capacity diverges to positive infinity above and negative infinity below the transition with the micro-canonical transition temperature approaching zero.

The basic mechanism responsible for the region of negative specific heat capacity, is super-exponential, or as we will find, near-exponential growth of degeneracies at low energies $k \lesssim N \log N$. At higher energies, finite N effects tame the rapid growth of degeneracies and the micro-canonical specific heat is positive.

It is natural to ask if the same mechanism exists in matrix or tensor systems of size N in the large N limit for cases with continuous symmetries such as $U(N)$. In the second part of the paper, we demonstrate that this is indeed the case. Our main results here are:

- We write down the path-integrals for complex tensors with indices transforming in a product of $U(N)$ groups. This allows us to derive the asymptotic divergence of the partition function near $x = 1$ and hence to count the number of physical degrees of freedom. For a system of d complex s tensors transforming under the group $U(N)^{\times s}$ we find for $d > 1$ and $s > 1$ that $N_{\text{phys}} = 2dN^s - s(N^s - 1) + 1$ (see (7.8)). We note that this number is known in mathematics as the Krull dimension of the commutative algebra of invariants, see [43].
- We find indications of similar thermodynamic characteristics to the gauged permutation invariant matrix model in a system with gauged $U(N)^{\times 3}$ acting on complex 3-index tensors. This includes a Hagedorn-like cross-over transition which is expected to vanish as N goes to infinity, in-equivalence between the canonical and

micro-canonical ensembles in the low temperature region, and negative specific heat capacity at low micro-canonical temperature. The evidence involves a combination of the high temperature behaviour we have derived from the path integral formulation, and computational evidence based on known group-theoretic formulae involving Kronecker coefficients (see eqn (8.7)) for the finite N counting of tensor model invariants. The SAGE code needed to do the computations is included in the discussion.

- We find indications of the features of in-equivalence of ensembles and negative specific heat capacity in the zero-charge sector of a complex one-matrix model (equivalently 2-Hermitian matrix model) having $U(N)$ gauge symmetry. This model has a finite temperature Hagedorn phase transition as N goes to infinity. The negative specific heat capacity, which is the heat capacity rescaled by $1/N^2$, at generic fixed temperatures below the Hagedorn temperature vanishes in the large N limit, but remains finite when the temperature is infinitesimally close to the Hagedorn temperature in the large N limit. The evidence again consists of the high temperature limit which is obtained from the path integral combined with computation with group-theoretic formulae for the counting in terms of Littlewood-Richardson coefficients (see eqn (9.23)). The SAGE code is again provided.
- Examples of small N canonical partition functions are presented for complex vectors (section 6.1), complex two tensors (section 6.2), the 3-tensor case (section 6.3), Hermitian matrices (section 6.4) and the charge zero sector of two matrix models (section 6.5). These are obtained by performing the contour integrals in the Molien-Weyl formula for the generating function of invariants to obtain explicit rational functions of $x = e^{-\beta}$.

The paper is organised as follows: We begin with a review of gauged permutation invariant matrix quantum mechanics (GPIMQM) in section 2. We review analytic expressions for the micro-canonical and the canonical partition functions for the simplest GPIMQM, where the quadratic potential is $\text{tr}(MM^T)$. This is a point of enhanced symmetry in the 11-dimensional parameter space of harmonic oscillator potentials considered in [33, 6, 7], where the Hamiltonian commutes with $U(N)$, but the state space includes S_N invariant polynomials in the oscillators.

In section 3 we discuss the thermodynamics of the simplest harmonic oscillator GPIMQM as a function of the temperature, conveniently parameterised by $x = e^{-\beta} = e^{-1/T}$, and matrix size N . Using the formula (2.15) we are able to compute the canonical partition functions for values of N up to around $N = 40$, with the help of Mathematica with computation times less than a minute to two hours. Some of our calculations take longer and extend to $N = 70$. We examine the expectation values of the energy, heat capacity and entropy. We establish that there is a Hagedorn crossover transition at finite N . This

occurs at decreasing temperatures as N is increased and goes to zero approximately as $x \sim x_c = \frac{\log N}{N}$. The specific heat capacity has a sharp peak in the transition region and remains positive for all x , as is required in the thermodynamics of a Hamiltonian system where the partition function $\text{tr}(e^{-\beta H})$ is well-defined (see (3.13)). The specific heat capacity has a maximum at $x = x_{\max} \sim x_c$ and there is a narrow critical region around it. It is easily seen that x_{\max} decreases as N increases, see Figure 2. A good fit to the data for large N is given by $x_{\max} = a \frac{\log N}{N} + \frac{b}{N} + c \frac{\log N}{N^2}$, with N -independent constants which we determine numerically with the help of Mathematica. The form of the ansatz follows the derivation of a formula for the scale of breakdown of the high temperature expansion in section 5. The fitted result is presented in Figure 17.

In section 4 we switch to a discussion of the GPIMQM system in the microcanonical ensemble. We find that the specific heat capacity in the low temperature region is negative. The negative sign is accompanied by an inequivalence between the canonical and micro-canonical ensembles in this low temperature region, as illustrated by Figure 15. The possibility of this type of inequivalence associated with a non-concave entropy function $S(U)$ in the micro-canonical ensemble has been discussed in the statistical physics literature e.g. [44] and the example at hand is aligned with these discussions. The region of inequivalence between ensembles, $x \lesssim x_c = \frac{\log N}{N}$, goes to zero in the large N limit. The two ensembles agree in the high temperature region above the cross-over transition.

In section 5 we derive the high temperature expansion and obtain a formula for the breakdown scale of the high temperature expansion, denoted x_{bkdn} by comparing the leading two terms. The leading term is associated with the partition $p = [1^N]$ (corresponding to the identity permutation) in the expansion for $\mathcal{Z}(N, x)$ in terms of partitions p (2.15). The next-to-leading term comes from $p = [2, 1^{N-2}]$. We refer to the preponderance of small parts, corresponding to small cycles in the cycle decomposition of these permutations, as small cycle dominance. The formula for the x_{bkdn} is a series involving powers of $\frac{\log N}{N}$ and $\frac{1}{N}$. The leading term $\frac{1}{2} \frac{\log N}{N}$ leads to the definition of $x_c = \frac{\log N}{N}$ which is found to also play an important role as a characteristic scale of the cross-over transition in the numerical study of the partition functions in sections 3 and 4.

Section 6 discusses the path integral formulation of vector and tensor models and we exhibit sample small N partition functions. Subsection 6.5 deals with the charge-zero sector of two matrix models. We derive a Molien-Weyl formula for the partition function and evaluate explicit expressions for partition functions for $N = 2, 3$ and 4 and the large N low temperature limit observing that in the micro-canonical ensemble this charge-zero system also exhibits negative specific heat (see section 9.2). Section 7 deals with the high temperature scaling in the path integral formulation.

In section 8 we combine information from the high temperature limits with representation theoretic formulae in two cases of interest, to deduce that there is a negative specific heat capacity at low temperature in the micro-canonical ensemble followed by a transition

and a high temperature phase of free oscillators. The two cases of primary interest involve a 3-index tensor system and a complex-matrix system with zero charge.

Section 9 presents a discussion of general forms of degeneracies leading to negative specific heat capacities along with connections with the physics of small black holes via the AdS/CFT correspondence. This discussion includes instances of multi-matrix thermodynamics which show negative specific heats when the number of matrices scales with the energy. We conclude with a summary of our results and a brief discussion of future research directions in section 10. The Appendices develop technical points arising in the main discussion.

2 Bosonic GPIMQM Partition functions : Review

In [7] we derived formulae for the partition functions of matrix harmonic oscillators with a general 11-parameter family of potentials invariant under the symmetric group S_N and with gauged S_N symmetry. The partition functions were expressed as sums over partitions of N . Each partition corresponds to a cycle structure of permutations in S_N . The summand associated to a given partition was given as a product involving the least common multiples (LCM) and greatest common divisors (GCD) of pairs of cycle lengths. In this paper, we focus on the case where the quadratic potential for the matrix variables M_{ij} with $i, j \in \{1, \dots, N\}$ is simply $\text{tr}(MM^T)$. We review the formula for the partition function here.

For permutations $\sigma \in S_N$, let U_σ be the linear operator acting in the natural representation V_N of S_N . Matrix bosonic oscillators A_{ij}^\dagger with $i, j \in \{1, 2, \dots, N\}$ admit an action of U_σ :

$$A_{ij}^\dagger \rightarrow (U_\sigma)_{ik} A_{kl}^\dagger (U_\sigma^T)_{lj} \quad (2.1)$$

or in matrix notation

$$A^\dagger \rightarrow U A^\dagger U^T. \quad (2.2)$$

The action can also be written as :

$$A_{ij}^\dagger \rightarrow A_{\sigma(i)\sigma(j)}^\dagger \quad (2.3)$$

The dimension of the subspace of the Fock space of these oscillators, at degree k , which is invariant under the S_N action has been computed in eqn (B.9) of [27]. The discussion in the paper [27] is in the context of polynomial functions of a classical matrix variable M_{ij} invariant under the action

$$M_{ij} \rightarrow M_{\sigma(i)\sigma(j)} \quad (2.4)$$

and the mathematics, of this invariant theory question, evidently applies equally well to the same action on bosonic oscillators.

The dimension of the space of S_N invariants at degree k is given as a sum of partitions of N and k

$$\mathcal{Z}(N, k) = \sum_{p \vdash N} \frac{1}{\text{Sym } p} \mathcal{Z}(N, p, k) \quad (2.5)$$

where

$$\mathcal{Z}(N, p, k) = \sum_{q \vdash k} \frac{1}{\text{Sym } q} \prod_i \left(\sum_{l|i} l p_l \right)^{2q_i}. \quad (2.6)$$

Define the generating function

$$\begin{aligned} \mathcal{Z}(N, x) &= \sum_{k=0}^{\infty} x^k \mathcal{Z}(N, k) \\ &= \sum_{k=0}^{\infty} \sum_{p \vdash N} \frac{x^k}{\text{Sym } p} \mathcal{Z}(N, p, k) \\ &= \sum_{p \vdash N} \frac{1}{\text{Sym } p} \sum_k x^k \mathcal{Z}(N, p, k) \end{aligned} \quad (2.7)$$

It is also useful to define a generating function for fixed N and fixed partition p of N by summing over k

$$\mathcal{Z}(N, p, x) = \sum_k x^k \mathcal{Z}(N, p, k) \quad (2.8)$$

$\mathcal{Z}(N, x)$ can therefore be written as a sum

$$\mathcal{Z}(N, x) = \sum_{p \vdash N} \frac{1}{\text{Sym } p} \mathcal{Z}(N, p, x) \quad (2.9)$$

For partitions of N the form $p = [a_1^{p_1}, a_2^{p_2}, \dots, a_s^{p_s}]$, where a_i are distinct non-zero parts with $1 \leq a_i \leq N$ and p_i are positive integers. It is often useful to think of the numbers to be ordered as $a_1 < a_2 < \dots < a_s$.

$$N = \sum_{i=1}^s a_i p_i \quad (2.10)$$

In [7] we derived the following formula for $\mathcal{Z}(N, p, x)$ which we refer to as the LCM formula:

$$\mathcal{Z}(N, p, x) = \prod_i \frac{1}{(1 - x^{a_i})^{a_i p_i^2}} \prod_{i < j} \frac{1}{(1 - x^{L(a_i, a_j)})^{2G(a_i, a_j) p_i p_j}} \quad (2.11)$$

$L(a_i, a_j)$ is the LCM of a_i and a_j and $G(a_i, a_j)$ is the GCD of a_i, a_j . A useful fact is that

$$a_i a_j = L(a_i, a_j) G(a_i, a_j) \quad (2.12)$$

The expression $2G(a_i, a_j)p_i p_j$ in (2.11) can also be written as :

$$2G(a_i, a_j)p_i p_j = \frac{2a_i a_j p_i p_j}{L(a_i, a_j)} \quad (2.13)$$

We can also present p as $[i^{p_i}]$ where i are all integers in the set $\{1, \dots, N\}$ and p_i are non-negative integers (possibly zero). In this case we can write

$$\mathcal{Z}(N, p, x) = \prod_i \frac{1}{(1 - x^i)^{ip_i^2}} \prod_{i < j} \frac{1}{(1 - x^{L(i,j)})^{2G(i,j)p_i p_j}} \quad (2.14)$$

The terms with $p_i = 0$ all give factors of 1 so this immediately reduces to the previous formula. In summary, a very useful formula for the canonical partition function is

$$\mathcal{Z}(N, x) = \sum_{p \vdash N} \frac{1}{\text{Sym } p} \prod_i \frac{1}{(1 - x^i)^{ip_i^2}} \prod_{i < j} \frac{1}{(1 - x^{L(i,j)})^{2G(i,j)p_i p_j}} \quad (2.15)$$

3 GPIMQ-thermodynamics in the canonical ensemble : finite N cross-over transition and vanishing Hagedorn temperature

The formula (2.15) for the generating function of permutation invariants of matrices reviewed above, allows a detailed study of the thermodynamics of a gauged permutation invariant quantum mechanical $N \times N$ matrix system of oscillators. In this section, we will focus on thermodynamics in the canonical ensemble. The variable x in the generating function is interpreted physically as $e^{-\beta}$ where $\beta = \frac{1}{T}$ is the inverse temperature. In the path integral formulation of the gauged permutation invariant matrix oscillator [6], β is the periodicity in the Euclidean time direction. The fixed energy degeneracies $\mathcal{Z}(N, k)$ have a very rapid super-exponential growth as a function of the energy k , when $N \geq 2k$. This is explained in section 3.1 below. Whereas the exponential degeneracies arising from multi-matrix models lead to a finite Hagedorn temperature (see e.g. [8][10]), super-exponential degeneracies lead to a vanishing Hagedorn temperature, as has been discussed recently in the context of tensor models [41][42].

In section 3.2 we give a brief review of the key formulae for the thermodynamic quantities in the canonical ensemble - energy, entropy and heat capacity - and describe the behaviour of these quantities as a function of temperature for a range of fixed values of N up to $N = 40$. Since the system under consideration is one of N^2 particles, subject to a

gauge symmetry constraint, it is natural to consider the energy, specific heat capacity and entropy divided by N^2 , which are obtained from $\frac{\log \mathcal{Z}(N,x)}{N^2}$ and its derivatives. We will refer to the heat capacity divided by N^2 as the specific heat capacity. These quantities are finite as $N \rightarrow \infty$ for generic x . We present numerical evidence that at $x \sim x_c = \frac{\log N}{N}$ there is a rapid cross-over in the energy and entropy curves, signalled by a specific heat capacity which scales like $N \log N$ (or heat capacity of $N^3 \log N$). An analytic derivation of the $\frac{\log N}{N}$ scale as the scale of breakdown of a high temperature expansion developed in 5, is given in section 5.2.

It should be noted that obtaining analogous closed form generating functions for continuous gauge symmetries such as $U(N)$ in the case of multi-matrix and tensor degrees of freedom is a challenging problem. For a nice review of matrix invariant theory see [43]. For example the two variable generating functions, for $U(N)$ invariants of 2-matrix systems, are given in [46] up to $N = 6$ and the single variable $N = 7$ case was evaluated in [10]. No larger N examples are available in print.

The high temperature limit of the permutation invariant thermodynamics is simple, since it is essentially that of N^2 free harmonic oscillators - the analytic formulae for this high temperature limit is reviewed in Appendix A. We conclude this section with a description of the zeroes of the partition function $\mathcal{Z}(N, x)$ in the complex plane : a set of closely spaced zeroes approaching the origin in the large N limit gives an additional perspective on the vanishing Hagedorn temperature. The role of such zeroes in connection with the finite temperature Hagedorn transition in 2-matrix systems has been given in [10].

3.1 Super-exponential degeneracies and vanishing Hagedorn temperature

The sequence of numbers $\mathcal{Z}(N, k)$, the dimensions of the vector space of S_N invariant polynomials in a matrix X of degree k , for fixed N and varying k has a universal behaviour for k up to $\frac{N}{2}$. This means that

$$\text{If } k \leq \frac{N}{2}, \quad \mathcal{Z}(N, k) = \mathcal{Z}(M, k) \quad \text{for all } M \geq N. \quad (3.1)$$

We may also write

$$\text{If } k \leq \frac{N}{2}, \quad \mathcal{Z}(N, k) = \mathcal{Z}(\infty, k) \equiv \lim_{M \rightarrow \infty} \mathcal{Z}(M, k). \quad (3.2)$$

We refer to $k \leq \frac{N}{2}$ as the stable region in the counting of S_N matrix invariants. This is analogous to the behaviour of the counting of $U(N)$ invariant polynomials in a matrix X of degree k which has a stable form for $k \leq N$, but for $k > N$ has corrections due to finite N relations (Caley-Hamilton relations). The existence of a stable region is a typical

property of the counting of multi-matrix and tensor invariants, of interest in multi-matrix models and tensor models.

The large N sequence for S_N invariants is given by directed multi-graphs with k edges (any number of nodes) [35]. The stable sequence $\mathcal{Z}(k, \infty)$ grows approximately as $k!$ at large k , by using the graph theoretic interpretation. The counting of directed multi-graphs is certainly as large as the counting of undirected graphs. The set of all undirected graphs with fixed number of edges includes the counting with fixed valency types. It is known [45] that the leading large k counting of graphs with k quartic vertices grows as $k \log k$, a fact familiar to quantum field theorists from the factorial growth of Feynman graph counting. Given such a growth of $\mathcal{Z}(k, \infty)$ as a function of k it is evident that

$$\sum_{k=0}^{\infty} \mathcal{Z}(k, \infty) e^{-\beta k} \quad (3.3)$$

diverges for any finite x or β , or equivalently any finite temperature. There is a similar growth of degeneracies in the stable region in the context of tensor models, and this has been interpreted as a zero-temperature Hagedorn transition [41] [42]. We will return to the tensor model case in more detail in sections 6 and 7.

The numerical studies in this section show that if we keep N finite, the partition function converges for finite temperatures, and has a sharp transition localised within a region of size $x \lesssim x_c = \frac{\log N}{N}$, which goes to zero as $N \rightarrow \infty$. We will explain this scaling of the transition region from the point of view of the high temperature expansion in section 3.3. In the next section 4, we will find that the region $x \lesssim \frac{\log N}{N}$ also displays the phenomenon of negative specific heat capacity and ensemble in-equivalence.

3.2 Thermodynamic quantities in the canonical ensemble

The canonical partition function is defined as a trace of the Hilbert space \mathcal{H}

$$\text{Tr}_{\mathcal{H}} e^{-\beta H} = \sum_{k=0}^{\infty} \mathcal{Z}(N, k) e^{-\beta k} = \mathcal{Z}(N, x) \quad (3.4)$$

where $x = e^{-\beta}$ and $\beta = \frac{1}{T}$ is the inverse temperature. The energy levels in this matrix harmonic oscillator system are non-negative integers and the degeneracies of the energy levels are dimensions of spaces of permutation invariant polynomials of degree k in matrix variables of size N .

We will define the dimensionless version \mathcal{W} of the Helmholtz free energy \mathcal{F} as

$$\mathcal{W} = -\beta \mathcal{F} = \log \mathcal{Z} \quad (3.5)$$

Dividing by N^2 we define the dimensionless free energy per particle

$$W = \frac{\mathcal{W}}{N^2} = \frac{1}{N^2} \log \mathcal{Z} \equiv \log Z \quad (3.6)$$

W is finite in the large N limit for generic x , i.e. W scales as N^2 .

The internal energy is the expectation value of the energy

$$\mathcal{U} = -\frac{1}{Z} \frac{\partial Z}{\partial \beta} \quad (3.7)$$

while the internal energy per particle is

$$U = \frac{\mathcal{U}}{N^2} = -\frac{1}{Z} \frac{\partial Z}{\partial \beta} = -\frac{\partial W}{\partial \beta} = \frac{x \partial W}{\partial x} \quad (3.8)$$

The heat capacity is

$$C_{\text{sh}} = \frac{\partial \mathcal{U}}{\partial T} \quad (3.9)$$

while the heat capacity per particle, or specific heat capacity

$$C_{\text{sh}} = \frac{\partial U}{\partial T} = \frac{1}{N^2} C_{\text{sh}} \quad (3.10)$$

is finite as $N \rightarrow \infty$ for generic T . The specific heat capacity is

$$\begin{aligned} C_{\text{sh}} &= \frac{\partial U}{\partial T} = \frac{\partial \beta}{\partial T} \frac{\partial U}{\partial \beta} \\ &= (\log x)^2 \left(x^2 \frac{\partial^2}{\partial x^2} W + x \frac{\partial}{\partial x} W \right) \\ &= (\log x)^2 \left(\frac{x^2}{Z} \frac{\partial^2 Z}{\partial x^2} - \frac{x^2}{Z^2} \left(\frac{\partial Z}{\partial x} \right)^2 + \frac{x}{Z} \frac{\partial Z}{\partial x} \right) \end{aligned} \quad (3.11)$$

It is also useful to write

$$\begin{aligned} C_{\text{sh}} &= -\beta \frac{\partial U}{\partial \beta} = \beta^2 \frac{\partial^2 W}{\partial \beta^2} \\ &= \beta^2 \frac{\partial}{\partial \beta} \left(\frac{1}{Z} \frac{\partial Z}{\partial \beta} \right) = \beta^2 \left(-\frac{1}{Z^2} \frac{\partial Z}{\partial \beta} \frac{\partial Z}{\partial \beta} + \frac{1}{Z} \frac{\partial^2 Z}{\partial \beta^2} \right) \\ &= \beta^2 (\langle H^2 \rangle - \langle H \rangle^2) \end{aligned} \quad (3.12)$$

The dispersion

$$\langle H^2 \rangle - \langle H \rangle^2 = \langle (H - \langle H \rangle)^2 \rangle \quad (3.13)$$

is positive. Thus we conclude that

$$C_{\text{sh}} \geq 0 \quad (3.14)$$

Note that this positivity of the specific heat capacity does not hold for the micro-canonical ensemble, as discussed in the literature on statistical thermodynamics, see [44] and references therein.

The probability of energy levels E at temperature T in canonical ensemble is given by

$$P(E, T) = \frac{1}{\mathcal{Z}} e^{\frac{-E}{T}} = e^{\frac{(-E+\mathcal{F})}{T}} \quad (3.15)$$

where the Helmholtz Free energy \mathcal{F} is defined in terms of the partition function \mathcal{Z} by

$$\mathcal{F} = -T \log \mathcal{Z} \quad (3.16)$$

The entropy in the canonical ensemble is defined as

$$\begin{aligned} \mathcal{S}(T) &= \langle \log P(E) \rangle = \frac{(E - \mathcal{F})}{T} = \log \mathcal{Z} + \frac{\mathcal{U}}{T} \\ &= \log \mathcal{Z} - \beta \frac{\partial \log \mathcal{Z}}{\partial \beta} = \log \mathcal{Z} - \log x \left(x \frac{\partial}{\partial x} \right) \log \mathcal{Z} \end{aligned} \quad (3.17)$$

In the case at hand we will be interested in

$$S = \frac{\mathcal{S}}{N^2} \quad (3.18)$$

which will be finite in the large N limit for generic x or generic β . In the canonical ensemble, approaching from $x \sim 1$ (corresponding to $\beta \rightarrow 0, T \rightarrow \infty$) towards $x \sim 0$ (corresponding to $\beta \rightarrow \infty, T \rightarrow 0$), we find a small region near $x \sim \frac{\log N}{N}$ where the high temperature expansion breaks down. In this region, vanishingly small as $N \rightarrow \infty$, the specific heat capacity rises to a very large value and then drops to zero.

3.2.1 Energy versus temperature

Figure 1 is a plot of the energy U as a function of $x = e^{-\beta}$ over the range $x \in [0, 1]$ which corresponds to $T \in [0, \infty]$, for $N = 20$. There is a sharp transition at $x \sim 0.1$ from low U to high U . In Figure 2 we have plotted the same curve for $N = 10, 15, 20$, demonstrating that the transition moves to lower x as N increases.

3.2.2 Specific heat capacity versus temperature

The Figure 3 shows a plot of the specific heat capacity C_{sh} as a function of x . There is a sharp peak at a critical $x \sim x_{\text{max}}$ which approaches zero temperature, corresponding to $x = 0$, as N increases. There is also a shallow minimum at $x > x_c$ followed by a monotonic rise towards $x \rightarrow 1$.

In section 5 we will derive an estimate of $x \sim x_c$ for the breakdown of the high temperature expansion

$$x_c = \frac{\log(N)}{N} \quad (3.19)$$

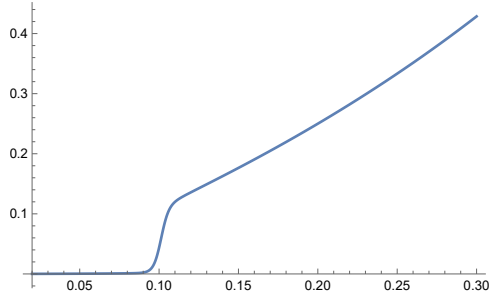


Figure 1: Energy versus temperature, parameterised by $x = e^{-\beta} = e^{\frac{-1}{T}}$ for $N = 20$: showing a cross-over

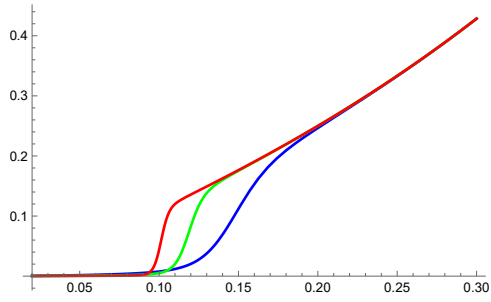


Figure 2: Energy versus temperature : Cross-over sharpens and approaches zero temperature as N increases. Blue, Green and Red curves are for $N = 10, 15, 20$

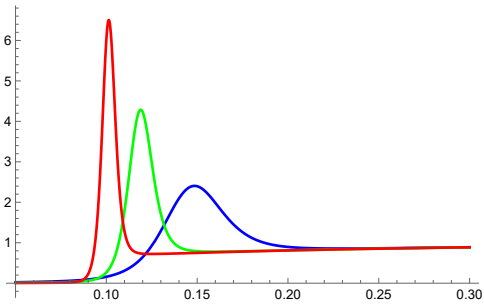


Figure 3: Specific heat capacity versus temperature : Sharp peak approaches zero temperature as N increases. Blue, Green and Red curves are for $N = 10, 15, 20$

Numerical plots show that, as expected, the high temperature expansion starts to deviate visibly from the exact partition function near the sharp transition region. This leads us to expect that the minimum and maximum of C_{sh} occur at locations $x_{\text{max}}, x_{\text{min}}$ which obey

$$\begin{aligned}\lim_{N \rightarrow \infty} \frac{x_{\text{max}}}{x_c} &= \text{finite} \\ \lim_{N \rightarrow \infty} \frac{x_{\text{min}}}{x_c} &= \text{finite}\end{aligned}\tag{3.20}$$

It is thus useful to define a_{max} and a_{min} by

$$\begin{aligned}x_{\text{max}} &= \frac{x_c}{a_{\text{max}}} \\ x_{\text{min}} &= \frac{x_c}{a_{\text{min}}}\end{aligned}\tag{3.21}$$

The data for $x_{\text{max}}, a_{\text{max}}$ for a number of sample values of N are as follows :

N	x_{max}	a_{max}
10	0.14855	1.55004
15	0.118935	1.51794
20	0.101350	1.47791
25	0.089096	1.44513
30	0.079880	1.41929
40	0.06654	1.38596

The data for $x_{\text{min}}, a_{\text{min}}$ are as follows :

N	x_{min}	a_{min}
10	0.22875	1.00659
15	0.159517	1.13177
20	0.124674	1.20143
25	0.104143	1.23633
30	0.0905245	1.2524

The value of the specific heat capacity at the maximum, although this is the heat capacity divided by N^2 (see equation (3.9)), has a peak which grows as N tends to infinity. We find that this maximum value which we denote as $C_{\text{sh};\text{max}}$ is of order 1 in units of $N \log N$ in the range of N up to 40, and conjecture that this will be the case as $N \rightarrow \infty$.

Conjecture 1:

$$\lim_{N \rightarrow \infty} \frac{C_{\text{sh};\text{max}}}{N \log N} = \text{finite}\tag{3.22}$$

Sample data illustrating the evidence which suggests this conjecture is

N	$\frac{C_{\text{sh};\text{max}}}{N \log N}$
10	0.104449
15	0.105513
20	0.108528
25	0.108454
30	0.106822
40	0.102552

On the other hand, the value of the specific heat capacity at the minimum, i.e. at $x = x_{\min}$, denoted $C_{\text{sh};\min}$ scales like $x_c = \frac{\log N}{N}$. This suggests the conjecture.

Conjecture 2:

$$\lim_{N \rightarrow \infty} \frac{C_{\text{sh};\min}}{x_c} = \lim_{N \rightarrow \infty} \frac{N C_{\text{sh};\min}}{\log N} = \text{finite} \quad (3.23)$$

A sample of the data suggesting this conjecture is

N	$\frac{C_{\text{sh};\min}}{x_c}$
10	3.72009
15	4.32296
20	4.82531
25	5.26598
30	5.66654
40	6.38326

It is also useful to tabulate the energy U , evaluated at x_{\min} and x_{\max} . In contrast to $C_{\text{sh};\max}$, and like $C_{\text{sh};\min}$, the natural scale for U in the transition region is, based on evidence from the data, $\frac{\log N}{N} = x_c$. In the following table we give the value $U_{\min} \equiv U(x_{\min})$:

N	$\frac{U_{\min}}{x_c}$
10	1.28359
15	1.04787
20	0.948274
25	0.900938
30	0.876539

Likewise the energy at the maximum $U_{\max} \equiv U(x_{\max})$ is given as:

N	$\frac{U_{\max}}{x_c}$
10	0.458389
15	0.412405
20	0.399507
25	0.395996
30	0.395297

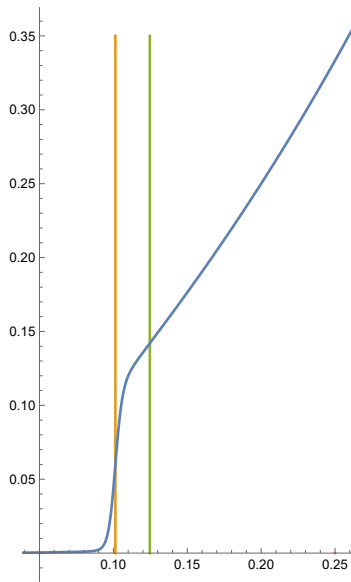


Figure 4: Energy curve showing location of x_{\max} (in yellow) at the centre of the energy transition region and x_{\min} (in blue) near the high temperature end of the transition. for $N = 20$.

The figure 4 illustrates the location of x_{\min} and x_{\max} relative to the sharp transition in the energy curve.

An interesting problem is to develop a model for these large N characteristics of the specific heat capacity and energy in the transition region, e.g. along the lines of [47].

3.2.3 Entropy versus temperature and Entropy as a function of Energy

As discussed at the start of this section, we calculate the entropy

$$S = \frac{1}{N^2} \left(\log \mathcal{Z} - \log x \left(x \frac{\partial}{\partial x} \right) \log \mathcal{Z} \right) \quad (3.24)$$

See the plot in Figure 6.

It is also natural to consider the entropy as a function of the energy E . To do this, we consider $E(T)$. This is a single-valued function, so we can invert it to obtain $T(E)$. The entropy as a function of E is then obtained from $S(T)$ by replacing T with $T(E)$:

$$S(E) = S(T(E)) \quad (3.25)$$

It will be instructive, in section 4, to compare this function of energy with the entropy in the micro-canonical ensemble.

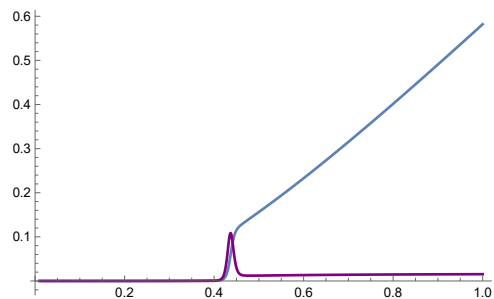


Figure 5: Energy per particle and specific heat capacity per particle divided by $N \log N$, plotted together versus temperature T at $N = 20$: illustrating macroscopic scale of the specific heat capacity in the transition region

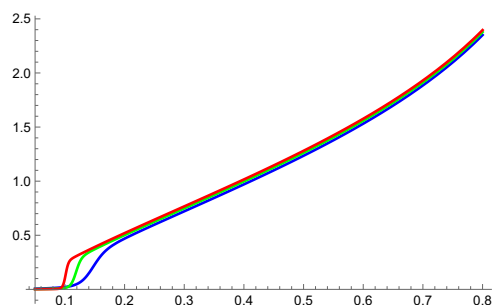


Figure 6: Entropy versus temperature : Sharp peak approaches zero temperature as N increases. Blue, Green and Red curves are for $N = 10, 15, 20$

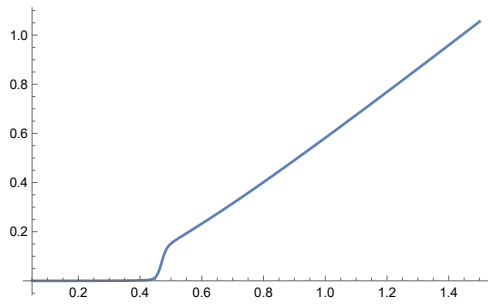


Figure 7: Energy versus temperature T at $N = 15$: Linear high temperature behaviour sets in near the high temperature end of the transition region

3.3 High temperature limit and N^2 simple harmonic oscillator thermodynamics

As we show in section 5 , the high temperature limit of the PIMQ thermodynamics is equivalent to that of N^2 particles in a harmonic oscillator. We recall the thermodynamic properties of this system in Appendix A. The energy U per particle is linear as a function of temperature T in the high temperature regime. This behaviour of U in the permutation invariant matrix oscillator is illustrated in Figure 7.

3.4 Zeroes in the complex plane

We get an interesting insight into the nature of the transition at $x \sim x_c$ by looking at the behaviour of $\mathcal{Z}(N, x)$ in the complex x -plane. See Figures 8 and 9. In both figures, there are a number of zeroes located close to a vertical line near $x = 0$. As N increases, the zeroes become closer to each other and to the origin $x = 0$. The table below gives the values of the zeroes nearest to the origin, for a range of N , illustrating how they approach the origin as N increases. They are tabulated alongside x_{\max} the location on the real x -axis of the maximum of the specific heat capacity C_{sh} in order to illustrate the proximity of these complex zeroes to the real temperature transition point. This proximity becomes sharper as N increases.

N	nearest zeroes in complex x -plane	x_{\max}
5	$0.20 \pm 0.13 i$	0.23
6	$0.18 \pm 0.09 i$	0.20
7	$0.17 \pm 0.07 i$	0.18
8	$0.16 \pm 0.05 i$	0.17
9	$0.15 \pm 0.04 i$	0.16

Note these zeroes are approaching the origin as $N \rightarrow \infty$. All the poles of $\mathcal{Z}(N, x)$ are on the unit circle. This is evident from plots and also from the expression 2.11.

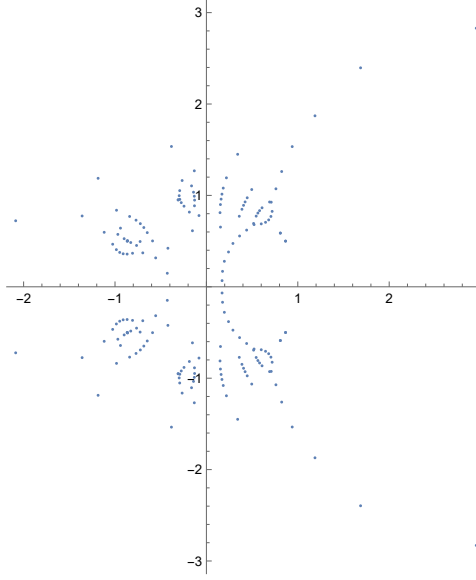


Figure 8: Zeroes of the canonical partition function in the complex x -plane for $N = 7$:
A line of zeroes approaches $x = 0$ as $N \rightarrow \infty$

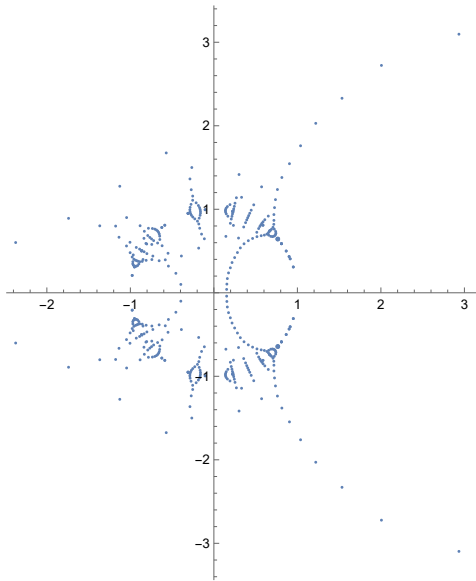


Figure 9: Zeroes of the canonical partition function in the complex x -plane for $N = 9$:
A line of zeroes approaches $x = 0$ as $N \rightarrow \infty$

4 PIMQ-Thermodynamics in the micro-canonical ensemble : Negative specific heat and (in)equivalence of ensembles

The canonical ensemble describes a physical system in equilibrium with thermal baths of fixed temperatures, as a function of the temperature. As reviewed in section 3.2 a notable feature of physics in the canonical ensemble is that the specific heat capacity is necessarily positive. In the micro-canonical ensemble, a system with discrete energy levels as is the system under study here, is considered in isolation as a function of the discrete values of the energy. In section 4.1, we review the key equations of thermodynamics in the micro-canonical ensemble and some relevant discussions of in-equivalence between the canonical and micro-canonical ensemble from the statistical physics literature.

We will use the coefficients in the expansion of $\mathcal{Z}(N, x)$, equation(2.15), to perform calculations in the micro-canonical ensemble. This is equivalent to but more efficient than using the original micro-canonical formula for $\mathcal{Z}(N, k)$ (equation (2.5)) in terms of a sum over partitions of N and k .

4.1 Micro-canonical ensemble and negative specific heat capacities

We will describe the translation between our generating functions $\mathcal{Z}(N, x)$ and $\mathcal{Z}(N, k)$ into thermodynamic quantities. k is the energy. $\mathcal{Z}(N, k)$ is the micro-canonical degeneracy. Following standard treatments of thermodynamics, the entropy as a function of energy is the logarithm of the degeneracy which is conventionally denoted $\Omega(N, k)$. Here these degeneracies are obtained as the coefficients $\mathcal{Z}(N, k)$ in the expansion of $\mathcal{Z}(N, x)$. Thus the micro-canonical entropy is

$$\mathcal{S}(N, k) = \log \mathcal{Z}(N, k) = \log \Omega(N, k) \quad (4.1)$$

We will occasionally emphasize that we are working with the micro-canonical ensemble rather than the canonical and will use $\Omega(N, k)$ for the degeneracies rather than $\mathcal{Z}(N, k)$. As in section 3, we define thermodynamic quantities per particle to obtain quantities with finite limits at generic x in the large N limit. The energy per particle is defined as $E = \frac{k}{N^2}$. Thus the micro-canonical entropy per particle is

$$S(N, E) = \frac{1}{N^2} \log \mathcal{Z}(N, k) = \frac{\mathcal{S}(N, N^2 E)}{N^2} \quad (4.2)$$

When we discuss equivalence and in-equivalence of micro-canonical and canonical ensemble, we will compare k in the micro-canonical ensemble to the expectation value \mathcal{U} (equation (3.7)) in the canonical ensemble, and equivalently in a per-particle comparison

we compare $E = \frac{k}{N^2}$ in the micro-canonical ensemble with $U = \frac{\mathcal{U}}{N^2}$ (equation (3.8)) in the canonical ensemble.

The temperature in the micro-canonical ensemble is defined as

$$T_{\text{micro}} = \left(\frac{\partial S}{\partial U} \right)^{-1} = \left(\frac{\partial \mathcal{S}}{\partial \mathcal{U}} \right)^{-1} \quad (4.3)$$

We use $\beta_{\text{micro}} = T_{\text{micro}}^{-1}$. Since the energy levels k are discrete with unit spacing, the micro-canonical temperature is defined using a discrete derivative Δ

$$T_{\text{micro}}^{-1}(k) = \frac{\Delta(\log(\mathcal{Z}(N, k)))}{\Delta k} \quad (4.4)$$

For Δ we will use D or D_{sym} where we define

$$DF(k) = F(k) - F(k-1) \quad (4.5)$$

or

$$D_{\text{sym}}F(k) = \frac{1}{2}(F(k+1) - F(k-1)) \quad (4.6)$$

which give

$$T_{\text{micro}}^{-1}(k) = (\log \mathcal{Z}(N, k) - \log \mathcal{Z}(N, k-1)) \quad (4.7)$$

or

$$T_{\text{micro;sym}}^{-1}(k) = \frac{1}{2}(\log \mathcal{Z}(N, k+1) - \log \mathcal{Z}(N, k-1)) \quad (4.8)$$

Defining the temperature using the entropy and energy per particle

$$T_{\text{micro}}^{-1}(k) = \frac{\Delta S}{\Delta E} = \frac{\Delta(\mathcal{S}/N^2)}{\Delta(k/N^2)} = \frac{\Delta(\log(\mathcal{Z}(N, k)/N^2))}{\Delta k/N^2} = \frac{\Delta(\log(\mathcal{Z}(N, k)))}{\Delta k} \quad (4.9)$$

which is the same as (4.4). In this form, it is clear that at large N , we are taking differences at points separated by vanishingly small separations, thus reaching a continuum limit.

4.2 Thermodynamic quantities in the micro-canonical ensemble

It is instructive to display the dependence of the thermodynamic quantities, notably the energy k and the specific heat capacity $C_{\text{sh;micro}}(T_{\text{micro}})$ in the micro-canonical ensemble.

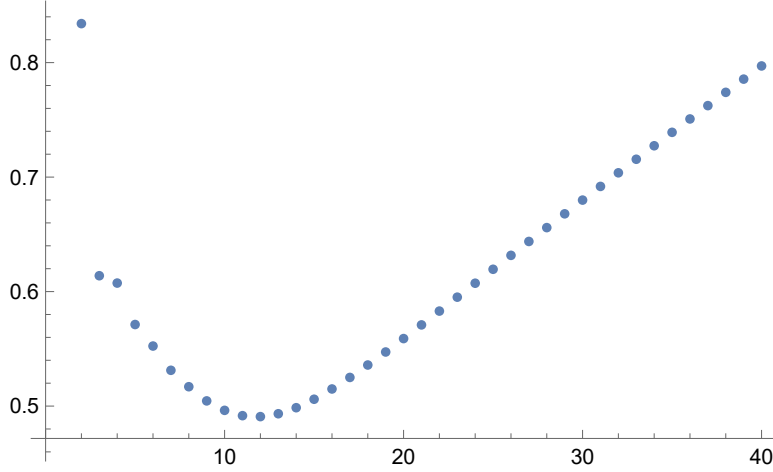


Figure 10: Plot of micro-canonical temperature k at $N = 10$ for $k_{max} = 40$ - using symmetrised derivative - produces consistent negative SHC trend below critical E

4.2.1 Energy versus micro-canonical temperature

Figure 11 shows a plot of $T_{\text{micro;sym}}(k)$ versus the energy k . The point ($k = 12, T = 0.491$) is at the minimum temperature. For lower temperatures the energy decreases as the energy increases. For $k \geq 12$, the energy increases with temperature. We will refer to this value of energy where the T_{micro} takes a minimum value as k_{crit} . Using the asymmetric discretisation of the derivative gives the same shape of curve. There are a couple of points at very small k where the variation of T_{micro} with k is different from that of $T_{\text{micro;sym}}$ with k . It is also useful to display the energy as a function of temperature, which will be useful later for comparison of the canonical and micro-canonical ensemble: see Figure 11. The micro-canonical specific heat capacity $\frac{\partial E}{\partial T_{\text{micro}}}$ tends towards negative infinity as k approaches k_{crit} from below and towards positive infinity as k approaches k_{crit} from above. Table 1 gives the values of k_{crit} for a range of values of N . All the integers in the second column are within ± 1 of $0.5N \log N$.

Conjecture 3: It is reasonable to conjecture that in the large N limit, the value of the un-normalised micro-canonical energy at the critical temperature where the specific heat capacity diverges, i.e k_{crit} , obeys

$$\text{Limit}_{N \rightarrow \infty} k_{\text{crit}} = 0.5 (N \log N) \quad (4.10)$$

The un-normalised energy is related to the number of edges in the graph in the graph theory interpretation reviewed briefly in section 3.1. With this conjecture, the critical energy per particle $E_{\text{crit}} = \frac{k_{\text{crit}}}{N^2}$ obeys

$$\text{Limit}_{N \rightarrow \infty} E_{\text{crit}} = 0.5 \frac{\log N}{N} \quad (4.11)$$

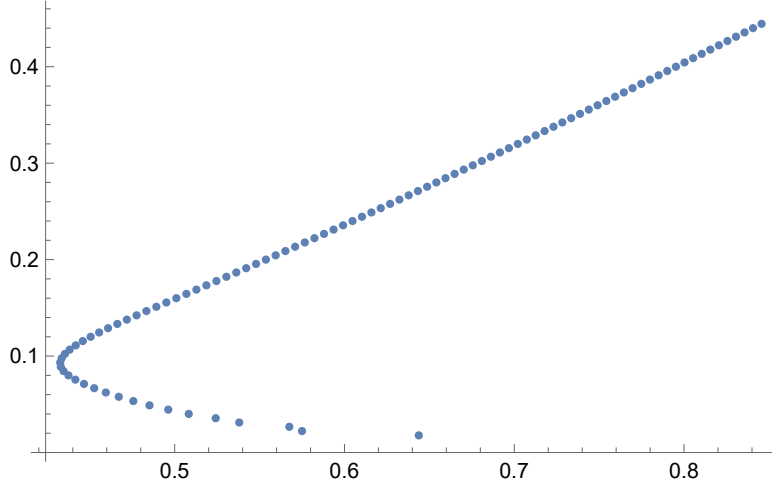


Figure 11: Plot of micro-canonical energy $\frac{E=k}{N^2}$ versus micro-canonical temperature at $N = 15$ for $k_{min} = 4, k_{max} = 100$ - using descending derivative - produces consistent negative SHC trend below critical E

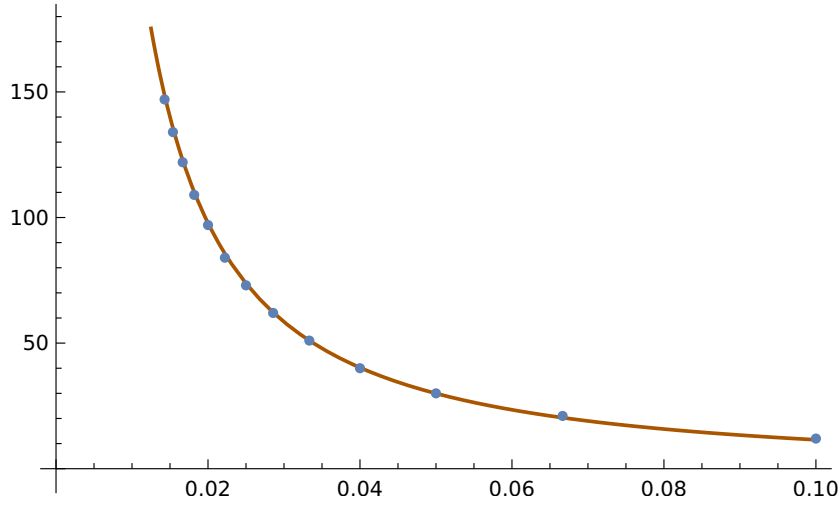


Figure 12: k_{crit} versus $\frac{1}{N}$ for $N = 10$ to $N = 70$. The curve is $\frac{1}{2} \frac{\log N}{N}$

Table 1: Table of values of k_{crit} as a function of N

N	k_{crit}	$\frac{k_{\text{crit}}}{N \log N}$
10	12	0.5212
15	21	0.5170
20	30	0.5007
25	40	0.4971
30	51	0.4998
35	62	0.4982
40	73	0.4947
45	84	0.4904
50	97	0.4959
55	109	0.4945
50	122	0.4966
65	134	0.4939
70	147	0.4943

4.2.2 Specific heat capacity versus micro-canonical temperature

From (4.3) we can calculate the derivative

$$\begin{aligned} \frac{\partial T_{\text{micro}}}{\partial E} &= -\frac{1}{\left(\frac{\partial S}{\partial E}\right)^2} \frac{\partial^2 S}{\partial E^2} \\ &= -\frac{1}{\left(\frac{1}{\Omega} \frac{\partial \Omega}{\partial E}\right)^2} \frac{\partial}{\partial E} \left(\frac{1}{\Omega} \frac{\partial \Omega}{\partial E} \right) \end{aligned} \quad (4.12)$$

The specific heat capacity is then

$$C_{\text{sh;micro}} = \frac{\partial E}{\partial T_{\text{micro}}} = -\left(\frac{1}{\Omega} \frac{\partial \Omega}{\partial E}\right)^2 \frac{1}{\frac{\partial}{\partial E} \left(\frac{1}{\Omega} \frac{\partial \Omega}{\partial E}\right)} \quad (4.13)$$

This can be expressed in terms of finite differences and plotted. The finite difference formula is

$$C = -\frac{(\Delta \log Z(k))^2}{\Delta(\Delta \log Z(k))} \quad (4.14)$$

The significant features are independent of the choice of discrete derivative. Calculations done with the two definitions are very close to each other except for very small k .

Figure 13 shows the negative specific heat separated from the region of positive specific heat, with the transition occurring at $E \sim \frac{\log N}{N}$. From (4.14), in negative SHC branch, the second derivative of the micro-canonical entropy as a function of energy is positive,

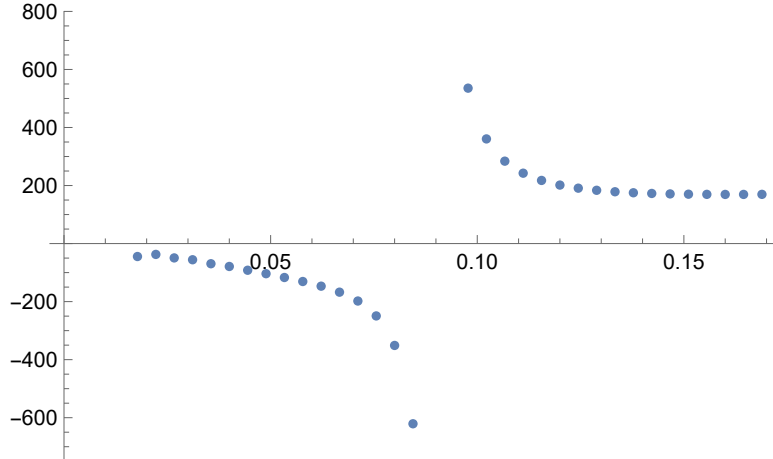


Figure 13: Plot of specific heat capacity versus E at $N = 15$

in other words, the entropy is convex. In the positive SHC branch the second derivative is negative, in other words the entropy is a concave function of the energy.

It is worth noting that when k exceeds $N/2$, we exit the stable regime of degeneracies described in (3.1) (3.2). However, at these low energies these departures from the stable regime do not cause a significant modification of the thermodynamic behaviour compared to the stable regime. A significant modification occurs at $k \sim N \log N$. This is analogous to a similar phenomenon discussed in the context of the thermodynamics of two matrix harmonic oscillators with $U(N)$ invariance. Here finite N trace relations lead to departures from stable behaviour at energies comparable to N , however thermodynamically significant departures occur for energies comparable to N^2 [48, 49].

4.3 Equivalence and in-equivalence of ensembles

The permutation invariant matrix quantum thermodynamics is well approximated by N^2 decoupled harmonic oscillators at high temperature. In this regime, we expect the micro-canonical ensemble and canonical ensemble to be equivalent. The thermodynamics of the multi-harmonic oscillator system along with an explicit account of ensemble equivalence in this context is discussed in Appendix A. Based on the general discussion of specific heat capacities in the canonical ensemble of statistical thermodynamics we have seen that these are related to a dispersion of the energy distribution and therefore positive (see (3.12)(3.13) (3.14)). As we observed in section 4.2.1 above, the micro-canonical entropy fails to be concave in the negative SHC region. This concavity plays a central role in the broad discussion of equivalence of ensembles in [44]. We therefore expect that in the region of T_{micro} where the SHC is negative, we have a failure of the equivalence between the canonical and micro-canonical ensemble.

In Figure 14 we have superposed for $N = 15$, a plot of the expectation value of the

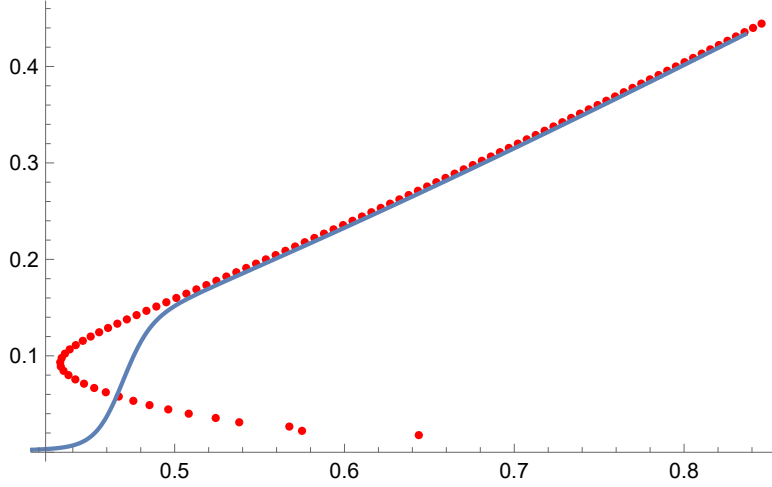


Figure 14: Plot of the expectation value of the energy $U = \mathcal{U}/N^2$ in the canonical ensemble versus canonical temperature T , superposed upon $E = \frac{k}{N^2}$ versus identification of T_{micro} in micro-canonical ensembles : Equivalence of ensemble above the transition region. This plot is for $N = 15$. The micro-canonical data starts at $k = 4$ and ends at $k = 100$.

energy per particle U in the canonical ensemble versus canonical temperature T with a plot of the rescaled per-particle energy level $E = \frac{k}{N^2}$ versus the micro-canonical temperature. This shows that, as expected, the two plots agree in the high temperature limit but disagree in the low temperature limit. Figure 15 gives the same superposition of plots at $N = 20$.

It is also instructive to perform a similar comparison for entropies. In the micro-canonical ensemble

$$S_{\text{micro}}(E) = \frac{1}{N^2} \log \Omega(E) = \frac{1}{N^2} \log \mathcal{Z}(N, k = N^2 E) \quad (4.15)$$

Expressing E as a function of T_{micro} , we can obtain a plot of $S_{\text{micro}}(T_{\text{micro}})$. As discussed around equations (3.24), we can also obtain an entropy function $S(T)$ for the canonical ensemble. Superposing $S_{\text{micro}}(T)$. Superposing these plots in Figure 16 we obtain the expected feature discussed above of ensemble in-equivalence at low temperature followed by equivalence at high temperature.

5 High temperature expansion of PIMQ-Thermo and small cycle dominance

In this section we will analyse the behaviour of the canonical partition function $\mathcal{Z}(N, x = e^{-\beta} = e^{-1/T})$ in the infinite temperature limit where $x \rightarrow 1$. The behaviour in this limit

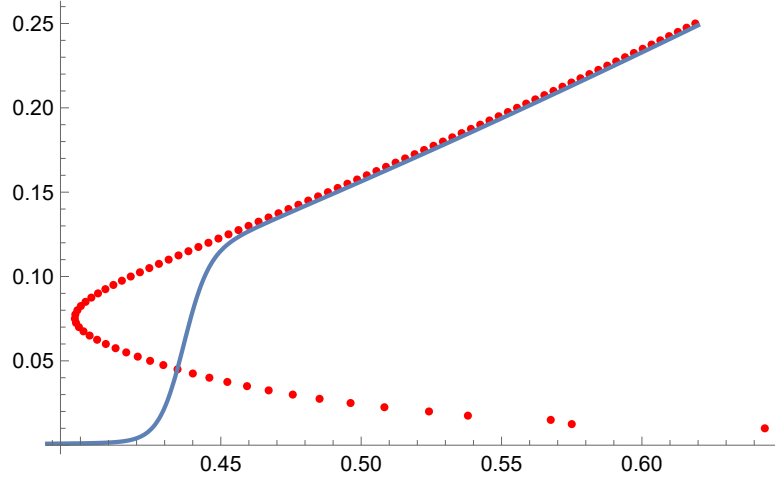


Figure 15: Plot of the expectation value of the energy $U = \mathcal{U}/N^2$ in the canonical ensemble versus canonical temperature T , superposed upon $E = \frac{k}{N^2}$ versus identification of T_{micro} in micro-canonical ensembles : Equivalence of ensemble above the transition region. This plot is for $N = 20$. The micro-canonical data starts at $k = 4$ and ends at $k = 100$.

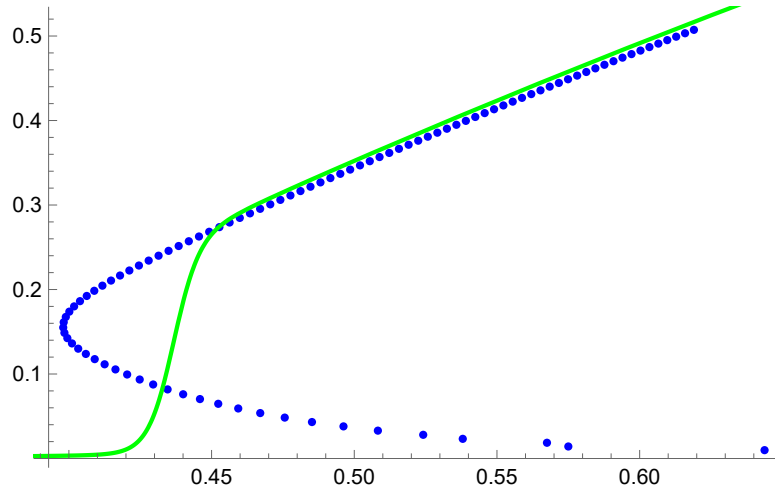


Figure 16: Plot of canonical ensemble entropy versus canonical temperature T superposed upon plot of micro-canonical entropy versus T_{micro} in the micro-canonical : Equivalence of ensemble above the transition region. This plot is for $N = 20$. The micro-canonical data starts at $k = 4$ and ends at $k = 100$.

is controlled by the singularity as $x \rightarrow 1$. Given that $\mathcal{Z}(N, x)$ is a sum over partitions p of $\mathcal{Z}(N, p, x)$ which, as we show, takes the form

$$\mathcal{Z}(N, p, x) = \frac{1}{(1-x)^{\text{Deg}(N, p)}} \mathcal{R}(x) \quad (5.1)$$

where $\text{Deg}(N, p)$ is an integer we will define and $\mathcal{R}(x)$ is a regular as $x \rightarrow 1$. We will show that the leading singularity of $\mathcal{Z}(N, x)$ as $x \rightarrow 1$ comes from $p = [1^N]$. The next-to-leading singularity come from $[1^{N-2}, 2]$, followed by other cycle structures involving a large number of 1-cycles and a few small cycles. The proof that $p = [1^N]$ gives the leading singularity follows, while the proof that the next-to-leading singularity comes from $p = [2, 1^{N-2}]$ is given in Appendix B.

We will start from (2.11) rewritten here for convenience

$$\mathcal{Z}(N, p; x) = \prod_i \frac{1}{(1-x^{a_i})^{a_i p_i^2}} \prod_{i < j} \frac{1}{(1-x^{L(a_i, a_j)})^{2G(a_i, a_j) p_i p_j}}$$

Note that

$$\frac{1}{(1-x^a)} = \frac{1}{(1-x)} \frac{1}{(1+x+x^2+\dots+x^{a-1})} \equiv \frac{1}{(1-x)} \mathcal{R}_a(x) \quad (5.2)$$

The residue

$$\text{Res}\left(\frac{1}{(1-x^a)}, x=1\right) = \mathcal{R}_a(x=1) = a^{-1} \quad (5.3)$$

This means that where we have separated the terms singular at $x=1$

$$\begin{aligned} \mathcal{Z}(N, p; x) &= \prod_i \frac{1}{(1-x)^{a_i p_i^2}} (\mathcal{R}_{a_i}(x))^{a_i p_i^2} \prod_{i < j} \frac{1}{(1-x)^{2G(a_i, a_j) p_i p_j}} (\mathcal{R}_{L(a_i, a_j)}(x))^{2G(a_i, a_j) p_i p_j} \\ &= \frac{1}{(1-x)^{\sum_i a_i p_i^2 + \sum_{i < j} 2G(a_i, a_j) p_i p_j}} \prod_i (\mathcal{R}_{a_i}(x))^{a_i p_i^2} \prod_{i < j} (\mathcal{R}_{L(a_i, a_j)}(x))^{2G(a_i, a_j) p_i p_j} \end{aligned} \quad (5.4)$$

5.1 Cycle structures and the high temperature expansion

We will define the degree function

$$\boxed{\text{Deg}(N, p) = \sum_i a_i p_i^2 + \sum_{i < j} 2G(a_i, a_j) p_i p_j} \quad (5.5)$$

which is the power of $(1-x)^{-1}$ in the formula (5.4). Note that

$$\text{Deg}(N, [1^N]) = N^2 \quad (5.6)$$

and for $p = [1^N]$

$$\frac{1}{\text{Sym } p} Z(N, p; x) = \frac{1}{N!} \frac{1}{(1-x)^{N^2}} \quad (5.7)$$

We will prove the following proposition

Proposition 1: The function

$$\text{Deg}(N, p) = \sum_i a_i p_i^2 + \sum_{i < j} 2G(a_i, a_j) p_i p_j \quad (5.8)$$

as p ranges over the set of partitions of N is maximised by $p = [1^N]$, where it takes values N^2 .

Before proving the result in general, we work out, by simple calculations, that the result holds for special classes of partitions. Consider partitions

$$p = [2^k, 1^{N-2k}] \quad (5.9)$$

In the notation of $p = [\{a_i^{p_i}\}]$

$$\begin{aligned} a_1 &= 1, p_1 = N - 2k, a_2 = 2, p_2 = k \\ G(a_1, a_2) &= 1 \end{aligned} \quad (5.10)$$

The degree is calculated as

$$\begin{aligned} \text{Deg}(N, [2^k, 1^{N-2k}]) &= (N - 2k)^2 + 2k^2 + 2 \cdot 1 \cdot k(N - 2k) = N^2 - 4Nk + 4k^2 + 2k^2 + 2kN - 4k^2 \\ &= N^2 - 2kN + 2k^2 \end{aligned} \quad (5.11)$$

For $k = 1$, we have $\text{Deg}(N, [2, 1^{N-2}]) = N^2 - 2N + 2$. Note that the coefficient of N is $-2B([2^k, 1^{N-2k}])$ where B is the branching number of the partition $[2^k, 1^{N-2k}]$. The branching number of a general partition $p = [\{a_i^{p_i}\}]$ is $\sum_i p_i(a_i - 1)$. It has an interpretation in terms of branched covers and plays a role in the Riemann-Hurwitz formula for the genus of covering surfaces in two dimensions. We will find shortly that this property, that the coefficient of N in the degree is the branching number of p , holds for general p .

For $p = [1^{N-2p_2-\dots-Kp_K}, a_2^{p_2}, a_3^{p_3}, \dots, a_K^{p_K}]$ with $p_2, p_3, \dots, p_K > 0$, $K < N$, we calculate the degree (5.5) to find

$$\begin{aligned} \text{Deg}(p, N) &= N^2 - 2N \left(\sum_{i=2}^K (a_i - 1) p_i \right) + \sum_{i=2}^K p_i^2 a_i (a_i - 1) + \sum_{i < j} 2p_i p_j (G(a_i, a_j) - a_i - a_j + a_i a_j) \\ &= N^2 - 2N \left(\sum_{i=2}^K (a_i - 1) p_i \right) + \sum_{i=2}^K p_i^2 a_i (a_i - 1) + \sum_{i < j} 2p_i p_j ((G(a_i, a_j) - 1) + (a_i - 1)(a_j - 1)) \end{aligned} \quad (5.12)$$

We can, without loss of generality, assume $a_2 < a_3 < \dots < a_K$.

Proof Using the definition of the degree in (5.5) and the form of p above

$$\begin{aligned}
\text{Deg}(p, N) &= (N - \sum_{i=2}^K a_i p_i)^2 + \sum_{i=2}^K a_i p_i^2 + \sum_{j=2}^K 2G(1, a_j)(N - \sum_{i=2}^K a_i p_i)p_j + \sum_{i < j} 2G(a_i, a_j)p_i p_j \\
&= N^2 - 2N \sum_{i=2}^K a_i p_i + (\sum_{i=2}^K a_i p_i)^2 + \sum_i a_i p_i^2 + \sum_{j=2}^K 2(N - \sum_i a_i p_i)p_j + \sum_{i < j} 2G(a_i, a_j)p_i p_j \\
&= N^2 - 2N \sum_{i=2}^K (a_i - 1)p_i + \sum_i a_i(a_i - 1)p_i^2 + 2 \sum_{i < j} a_i a_j p_i p_j \\
&\quad - 2 \sum_{j=2}^K a_j p_j^2 - 2 \sum_{i < j} p_i p_j (a_i + a_j) + 2 \sum_{i < j} G(a_i, a_j)p_i p_j \\
&= N^2 - 2N \sum_{i=2}^K (a_i - 1)p_i + \sum_{i=2}^K a_i(a_i - 1)p_i^2 + \sum_{i < j} 2p_i p_j (G(a_i, a_j) + a_i a_j - a_i - a_j) \\
&= N^2 - 2N (\sum_{i=2}^K (a_i - 1)p_i) + \sum_{i=2}^K p_i^2 a_i(a_i - 1) + \sum_{i < j} 2p_i p_j ((G(a_i, a_j) - 1) + (a_i - 1)(a_j - 1))
\end{aligned} \tag{5.13}$$

We have used $G(1, a_j) = 1$.

Note that the coefficient of $(-2N)$ is the branching number of p , denoted $B(p)$, which obeys $0 \leq B(p) \leq (N - 1)$. To see this note that

$$B(p) = \sum_{i=2}^N (a_i - 1)p_i = \sum_{i=1}^N (a_i - 1)p_i = N - \sum_{i=1}^N p_i \tag{5.14}$$

which is minimised when all the $a_i = 1$ (i.e $p = [1^N]$) and maximised when $p_N = 1$ with all other p 's zero, i.e. $p = [N]$. When $K, a_i, p_i \ll N$, the significant term is $-2NB(p)$, and it is evident that the largest degree term is the one where the $p_2 \dots p_K$ are all zero, and $B(p)$ which means that the degree is maximised by $p = [1^N]$. We can also relax this restriction $K, a_i, p_i \ll N$ and prove the desired maximisation property of $p = [1^N]$.

We know that

$$N > \sum_{i=2}^K (a_i - 1)p_i \tag{5.15}$$

This holds because the number of 1-cycles in p is greater or equal to 0 :

$$N - \sum_{i=2}^K a_i p_i \geq 0 \tag{5.16}$$

which means

$$N - \sum_{i=1}^K (a_i - 1)p_i > 0 \quad (5.17)$$

We can extend this by including $a_1 = 1$ and $p_1 = N - \sum_{i=2}^K a_i p_i$ so that

$$N - \sum_{i=1}^K (a_i - 1)p_i > 0 \quad (5.18)$$

The inequality (5.15) has the geometrical interpretation that the branching number of a branch point for an N -sheeted cover of a two dimensional surface can be at most $(N - 1)$. It is useful to write

$$\text{Deg}(p, N) = N^2 + \tilde{X}(N, \vec{a}) \quad (5.19)$$

where \tilde{X} is read off from (5.12) as

$$\tilde{X}(N) = -2N \left(\sum_{i=2}^K (a_i - 1)p_i \right) + \sum_{i=2}^K p_i^2 a_i (a_i - 1) + \sum_{i < j} 2p_i p_j ((G(a_i, a_j) - 1) + (a_i - 1)(a_j - 1)) \quad (5.20)$$

Our desired inequality is

$$\tilde{X}(N) < 0 \quad (5.21)$$

Given the inequality (5.15), it follows that if we replace $N \rightarrow \sum_{i=2}^K (a_j - 1)p_j$ in $\tilde{X}(N)$ to give $\tilde{X}(N, \vec{a}) \rightarrow X(\vec{a})$, we have the inequality $\tilde{X} < X$. Therefore proving $X < 0$ will prove (5.21).

The explicit form of $X(\vec{a})$ is

$$X = -2 \sum_{j=2}^K (a_j - 1)p_j \sum_{i=2}^K (a_i - 1)p_i + \sum_{i=2}^K p_i^2 a_i (a_i - 1) + \sum_{2 \leq i < j \leq K} 2p_i p_j ((G(a_i, a_j) - 1) + (a_i - 1)(a_j - 1)) \quad (5.22)$$

To prove $X < 0$, we simplify

$$X = -2 \sum_i p_i^2 (a_i - 1)^2 - 2 \sum_{i < j} p_i p_j ((a_i - 1)(a_j - 1) - (G(a_i, a_j) - 1))$$

$$= -2 \sum_i p_i^2 (a_i - 1)^2 - 2 \sum_{i < j} p_i p_j (a_i - 1)(a_j - 1) + 2 \sum_{i < j} p_i p_j (G(a_i, a_j) - 1) \quad (5.23)$$

The GCD satisfies $G(a_i, a_j) \leq a_i$, so

$$X < -2 \sum_i p_i^2 (a_i - 1)^2 - 2 \sum_{i < j} p_i p_j (a_i - 1)(a_j - 1) + 2 \sum_{i < j} p_i p_j (a_i - 1) \equiv X_1 \quad (5.24)$$

We simplify

$$X_1 = -2 \sum_i p_i^2 (a_i - 1)^2 - 2 \sum_{i < j} p_i p_j (a_i - 1)(a_j - 2) \quad (5.25)$$

We have, by assumption, $i \geq 2$, $a_i, a_j \geq 2$ and with $a_j > a_i$ we know $a_j \geq 3$ in the second sum above. This means

$$X_1 \leq -2 \sum_i p_i^2 (a_i - 1)^2 - 2 \sum_{i < j} p_i p_j (a_i - 1) \equiv X_2 \quad (5.26)$$

Now it is evident that $X_2 < 0$. Combining with $\tilde{X} < X < X_1 \leq X_2 < 0$, we conclude $\tilde{X} < 0$,

This proves the proposition.

5.2 Breakdown of the high T expansion and the characteristic scale $x_c = \frac{\log N}{N}$.

The degree function of the partitions can be easily computed in Mathematica and shows that the second most singular term at $x = 1$, after $[1^N]$ comes from $[2, 1^{N-2}]$. We have checked this for N up to 25 and give the proof for general N in Appendix B. We proceed here to investigate the implications for the nature of the transition region. The two leading terms in the high temperature expansion thus define a truncated partition function we denote Z_{trunc} .

$$\begin{aligned} \mathcal{Z}_{\text{trunc}}(N, x) &= \frac{1}{N!(1-x)^{N^2}} + \frac{1}{2(N-2)!} \frac{1}{(1-x)^{(N-2)^2} (1-x^2)^{2N-2}} \\ &= \frac{1}{N!(1-x)^{N^2}} \left(1 + \frac{N(N-1)}{2} \frac{(1-x)^{2N-2}}{(1+x)^{2N-2}} \right) \\ &= \frac{1}{N!(1-x)^{N^2}} \left(1 + \frac{N(N-1)}{2} \left(\tanh \frac{\beta}{2} \right)^{2N-2} \right) \end{aligned} \quad (5.27)$$

To get an estimate of the breakdown scale x_{bkdn} of the high temperature expansion, we set

$$\frac{N(N-1)}{2} \frac{(1-x_{\text{bkdn}})^{2N-2}}{(1+x_{\text{bkdn}})^{2N-2}} = a \quad (5.28)$$

where a is a small number $a < 1$, but a does not depend on N . This is solved by

$$x_{\text{bkdn}} = \tanh\left(\frac{B}{2}\right) = \frac{B}{2} - \frac{B^3}{24} + \dots \quad (5.29)$$

where

$$B = \frac{1}{2N} \left(1 - \frac{1}{N}\right) \left(2 \log N + \log\left(1 - \frac{1}{N}\right) + \log 2 - \log a\right) \quad (5.30)$$

The expansion of x_{bkdn} is a series in powers of the variables $\frac{\log N}{N}, \frac{1}{N}$ with constant coefficients. The first few terms are

$$x_{\text{bkdn}} = \frac{\log N}{2N} + \frac{1}{4N} (\log 2 - \log a) + \frac{1}{4N^2} (\log(\frac{a}{2}) - 1) - \frac{\log N}{2N^2} + \mathcal{O}\left(\frac{1}{N^3}\right) + \mathcal{O}\left(\frac{\log N}{N^3}\right) \quad (5.31)$$

Note that the first term $\frac{\log N}{2N}$ is independent of a . We will define $x_c = \frac{\log N}{N}$ as the characteristic scale of the transition. This scale has played an important role in the tables given in sections 3 and 4, where the characteristics of the transition measured in units of x_c show good evidence of being numbers of order 1 as $N \rightarrow \infty$.

Developing further the applications of x_c and x_{bkdn} , we present Figure 17 where we use the data from Tables 1 and 3.2.2 and fit the corresponding critical value of x against $1/N$. The data shows that the critical temperatures are driven to zero as expected and established by the high temperature analysis. The figure shows that the microcanonical transition is consistently at a lower temperature than the canonical one as expected from Figure 15 but both go to zero at infinite N as expected from the known stable structure of the degeneracies and from our high temperature analysis which establishes that the transition has to occur for $x \lesssim x_c = \frac{\log N}{N}$. Our fitting curves are motivated by the functional form suggested by the first three terms in 5.31.

6 Path Integral for Tensor Models

In this section we give the path integral formula for the thermal partition function of d copies of s -index tensors, as an application of [6]. This is used to derive a palindromy property for the canonical partition function by considering a transformation $x \rightarrow x^{-1}$, and to compute a number of explicit examples of the partition functions. In the next section, we obtain the high temperature limit from the path integral.

Let $\Phi_{i_1 \dots i_d}^a$, $a = 1, \dots, d$ be a set of tensors with each index transforming in the fundamental of distinct $U(N)$ groups, i.e. they transform under $U(N)^s$. The Euclidean thermal action for this system is then

$$S[\overline{\Phi}, \Phi] = \int_0^\beta d\tau \left((\mathcal{D}_\tau \overline{\Phi}_{i_1 \dots i_s}^a (\mathcal{D}_\tau \Phi^a)^{i_1 \dots i_s} + m_B^2 \overline{\Phi}_{i_1 \dots i_s}^a \Phi^{a i_1 \dots i_s} \right) \quad (6.1)$$

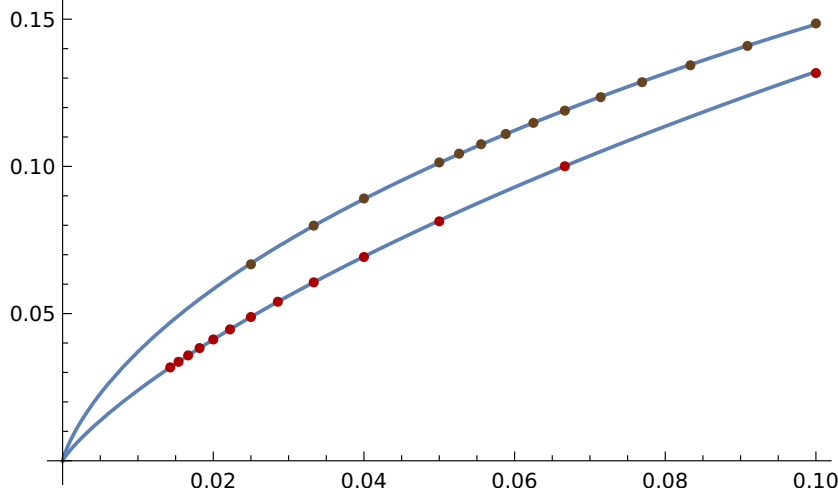


Figure 17: Comparison of microcanonical and canonical values for the transition value of $x = e^{-\beta}$ with $\beta = \beta_{micro}(k_{crit})$ for the microcanonical ensemble. The best fit curves, plotted against $\nu = \frac{1}{N}$ are $x_{crit}(\nu) = -0.508\nu \log(\nu) + 0.032\nu - 0.522\nu^2 \log(\nu)$ for the microcanonical ensemble and $x_{max}(\nu) = -2.86538\nu - 1.37557\nu \log(\nu) - 5.1274\nu^2 \log(\nu)$ for the canonical ensemble.

where $\mathcal{D}_\tau = \partial_\tau - iA$ is the covariant derivative with the gauge field $A(\tau) = \sum_{r=1}^s A^r(\tau)$ being a Hermitian matrix in the Lie algebra of $U(N)^s$. A subtlety associated with this system is that though the gauge group is $U(N)^s$ only $SU(N)^s \otimes U(1)$ has a non-trivial action on the tensors i.e. there is only a single $U(1)$ gauge field. The remaining $U(1)^{s-1}$ decouple completely from the system. The reason is rather straightforward: $U(N)$ can always be factored into $SU(N)$ and an overall $U(1)$ phase. But the s overall phases act as a single phase, yielding a single diagonal $U(1)$ action. The $U(1)$ gauge fields A_k are proportional to the identity matrix and therefore do not rotate the tensor's index, therefore they combine into with their sum $A_1 + \dots + A_s$ which is the effective $U(1)$ gauge field.

By taking a lattice gauge theory approach we have shown [6] that all the gauge group elements can be accumulated on a single link to give a holonomy element around the thermal circle and that the continuum partition function, after removing the zero point energy, $\prod_{a=1}^d x_a^{N^s}$, is given by the Molien-Weyl form

$$Z_N^{(s)}(x_1, \dots, x_d) = \int \mu(g_1) \dots \mu(g_s) \prod_{a=1}^d \frac{1}{\det[\mathbf{1} - x_a g_1 \otimes \dots \otimes g_s]} \frac{1}{\det[\mathbf{1} - x_a g_1^{-1} \otimes \dots \otimes g_s^{-1}]} \quad (6.2)$$

Here it is convenient to leave the $U(1)$ gauge fields that act trivially in the system. They simply do not contribute as their integrals automatically give one.

Diagonalization of a $U(N)$ group element g reduces it to the Cartan torus with eigen-

values $z_i = e^{i\theta_i}$ and the measure becomes a product of Vandermonde determinants

$$\Delta(z) = \prod_{1 \leq i < j \leq N} (z_i - z_j) \text{ and } |\Delta(z)|^2 = \Delta(z)\Delta\left(\frac{1}{z}\right). \quad (6.3)$$

The partition function (6.2) then becomes a set of contour integrals so that

$$Z_N^{(s)}(x_1, \dots, x_d) = \frac{1}{(N!)^s} \oint \prod_{r=1}^s |\Delta(z^r)|^2 \prod_{a=1}^d \prod_{i_1 \dots i_s=1}^N \frac{1}{|1 - x_a z_{i_1}^1 \dots z_{i_s}^s|^2}. \quad (6.4)$$

The integration is a contour integral $\oint \frac{dz}{2\pi iz}$ for each of the $N \times s$ Cartan torus variables z_i^s .

Explicitly for a set of d complex vectors Φ_i^a transforming under the group $U(N)$ we have

$$Z_N^{(1)}(x_1, \dots, x_d) = \frac{1}{(N!)} \oint |\Delta(z)|^2 \prod_{a=1}^d \prod_{i=1}^N \frac{1}{(1 - x_a z_i)(1 - \frac{x_a}{z_i})} \quad (6.5)$$

and for a set of d two-tensors Ψ_{ij}^a with transformation group $U(N) \times U(N)$ we have

$$Z_N^{(2)}(x_1, \dots, x_d) = \frac{1}{(N!)^2} \oint |\Delta(z)\Delta(w)|^2 \prod_{a=1}^d \prod_{i=1}^N \prod_{j=1}^N \frac{1}{(1 - x_a z_i w_j)(1 - \frac{x_a}{z_i w_j})} \quad (6.6)$$

and finally for the 3-tensor system Ψ_{ijk}^a with transformation group $U(N) \times U(N) \times U(N)$ we get

$$Z_N^{(3)}(x_1, \dots, x_d) = \frac{1}{(N!)^3} \oint |\Delta(z)\Delta(v)\Delta(w)|^2 \prod_{a=1}^d \prod_{i=1}^N \prod_{j=1}^N \prod_{k=1}^N \frac{1}{(1 - x_a z_i v_j w_k)(1 - \frac{x_a}{z_i v_j w_k})}. \quad (6.7)$$

When $x^a = x$, so that all x^a are equal, there is an additional $SO(d)$ symmetry and the resulting partition functions take the form

$$Z_N^{(s)}(x; d) = \frac{P_{N,K}^{(s)}(x; d)}{Q_{N,L}^{(s)}(x; d)} \quad (6.8)$$

with $P_{N,K}^{(s)}(x; d)$ and $Q_{N,L}^{(s)}(x; d)$ polynomials of degree K and L respectively. Also, assuming $x < 1$ one has the inversion relation

$$Z_N^{(s)}\left(\frac{1}{x}; d\right) = (-1)^{sN-n_0} x^{2dN^s} Z_N^{(s)}(x; d) \quad (6.9)$$

and the $(-1)^{sN-n_0}$ comes from reversing the contours, i.e. the transformation of $\frac{dz^{-1}}{z^{-1}} = -\frac{dz}{z}$ in the Molien-Weyl formula, when returning it to its original form and n_0 is the number of integrations that decouple completely. For $s > 1$ and $d > 1$ we have $n_0 = s-1$. Here

we see that $L - K = 2dN^s$ is the number of oscillators in the system. The multi-variable case satisfies a similar relation when x_a are inverted with $\prod_{a=1}^d x_a^{N^s} Z_N^{(3)}(x_1, \dots, x_d)$ transforming only by a sign. Due to the inversion relation, the polynomial $P_{N,K}^{(s)}(x, d)$ has palindromic coefficients modulo signs.

The transformation of $Z_N^{(s)}(x_1, \dots, x_d)$ follows from the path integral (6.1), which automatically includes the zero-point energy prefactor, by observing that $\beta m_a \rightarrow -\beta m_a$, which sends $x_a \rightarrow \frac{1}{x_a}$ is an invariance of the thermal action. What is less obvious is the phase factor, but this can be obtained from the high temperature analysis below.

The expressions (6.5) (6.6) (6.7) can be evaluated exactly for small N and d and we exhibit some illustrative results below.

6.1 Complex-Vectors

For small N and d the vector case can be evaluated explicitly to give for $d = 2$ and $N = 1$

$$Z_1^{(1)}(x, y) = \frac{1 - x^2 y^2}{(1 - x^2)(1 - y^2)(1 - xy)^2}. \quad (6.10)$$

One can easily work out $Z_1^{(1)}(x; d)$ for higher d to find

$$Z_1^{(1)}(x; d) = \frac{P_{1,2d-2}^{(1)}(x; d)}{(1 - x^2)^{2d-1}} \quad (6.11)$$

where $P_{1,2d-2}^{(1)}(x; d)$ is a palindromic even polynomial of degree $2d - 2$, e.g. $P_{1,2}^{(1)}(x; 3) = 1 + x^2$, $P_{1,4}^{(1)}(x; 4) = 1 + 4x^2 + x^4$ and $P_{1,6}^{(1)}(x; 3) = 1 + 9x^2 + 9x^4 + x^6$.

For N -component complex vectors with $N > 1$ we find

$$Z_N^{(1)}(x, y) = \frac{1}{(1 - x^2)(1 - y^2)(1 - xy)^2}. \quad (6.12)$$

For $d = 3$ with $U(2)$ gauge invariance we get

$$Z_2^{(1)}(x_1, x_2, x_3) = \frac{1 - x_1^2 x_2^2 x_3^2}{(1 - x_1^2)(1 - x_2^2)(1 - x_3^2)(1 - x_1 x_2)^2(1 - x_2 x_3)^2(1 - x_3 x_1)^2} \quad (6.13)$$

a result which indicates that the 9 invariants formed from the products of a Φ_i^a and $\bar{\Phi}^{bi}$ are not all independent and expanding the denominator overcounts the invariants. The overcounting is compensated for by the subtraction indicated in the numerator. The implied relation between invariants follows from the vanishing determinant of the 3×3 matrix of quadratic invariants.

Setting $x^a = 0$ for $a > 1$ reduces to the single vector case which can be evaluated in general to find

$$Z_N^{(1)}(x) = \frac{1}{1 - x^2}. \quad (6.14)$$

i.e. all invariants are formed from powers of the inner product of the vector with its conjugate, $\bar{\Phi} \cdot \Phi$. In the 2 vector case there are four basic invariants $\bar{\Phi}^1 \cdot \Phi^1$, $\bar{\Phi}^2 \cdot \Phi^1$, $\bar{\Phi}^1 \cdot \Phi^2$ and $\bar{\Phi}^2 \cdot \Phi^2$ and all other invariants are polynomials in these.

For general d with $d < N$ we obtain

$$Z_N^{(1)}(x_1, x_2, \dots, x_d) = \frac{1}{\prod_{a=1}^d (1 - x_a^2) \prod_{a < b=1}^d (1 - x_a x_b)^2} \quad (6.15)$$

so that in the $SO(d)$ symmetric case with all $x_a = x$ one gets

$$Z_N^{(1)}(x, d) = \frac{1}{(1 - x^2)^{d^2}}, \quad (6.16)$$

for all $d \leq N$. For $d > N$ the situation is more complicated as is indicated by the general scaling near $x = 1$, i.e. at asymptotically large temperatures, see 7.2.1.

6.2 Two-Tensors

For the two-index tensor case one can evaluate the contour integrals explicitly for all N with $d = 1$ finding

$$Z_N^{(2)}(x) = \prod_{n=1}^N \frac{1}{(1 - x^{2n})}. \quad (6.17)$$

One recognises that the invariants are built from traces of $X_i^j = \Psi_{ik} \bar{\Psi}^{kj}$ or equivalently the eigenvalues of X_i^j whose square roots are the singular values of Ψ_{ij} and the problem reduces to counting the invariants of a single matrix. So the invariants are the singular values of the 2-tensor, which can be thought of as a generic complex two matrix.

For a set of two tensors Ψ_{ij}^1 and Ψ_{ij}^2 one can again evaluate the partition function finding

$$Z_2^{(2)}(x, y) = \frac{(1 + x^2 y^2)(1 + x y^3 + 2x^2 y^2 + x^3 y + x^4 y^4)}{(1 - x^2)(1 - x^4)(1 - y^2)(1 - y^4)(1 - xy)^2(1 - x^2 y^2)(1 - xy^3)(1 - x^3 y)}, \quad (6.18)$$

which when reduced to the rotationally invariant case

$$Z_2^{(2)}(x; 2) = \frac{(1 + x^4)(1 + 4x^4 + x^8)}{(1 - x^2)^4(1 - x^4)^5}. \quad (6.19)$$

For three and more tensors the multi-variable results become increasingly more complicated and we quote only the rotationally invariant case for $d = 3$ where we find

$$Z_2^{(2)}(x; 3) = \frac{P_{2,28}^{(2)}(x; 3)}{(1 - x^2)^8(1 - x^4)^9} \quad (6.20)$$

and $P_{2,28}^{(2)}(x; 3)$ is the palindromic polynomial

$$P_{2,28}^{(2)}(x; 3) = 1 + x^2 + 37x^4 + 56x^6 + 353x^8 + 389x^{10} + 1037x^{14} + 704x^{14} + 1037x^{16} + 389x^{18} + 353x^{20} + 56x^{22} + 37x^{24} + x^{26} + x^{28} \quad (6.21)$$

while for $U(3)$ we get

$$Z_3^{(2)}(x; 2) = \frac{P_{3,48}^{(2)}(x; 2)}{(1-x^2)^3(1-x^4)^9(1-x^6)^7} \quad (6.22)$$

where $P_{3,48}(x; 2)$ is again an even palindromic polynomial of degree 48 given by

$$P_{3,48}^{(2)}(x; 2) = 1 + x^2 + 2x^4 + 19x^6 + 45x^8 + 78x^{10} + 208x^{12} + 426x^{14} + 621x^{16} + 911x^{18} + 1328x^{20} + 1507x^{22} + 1490x^{24} + \dots \quad (6.23)$$

6.3 Three-Tensors

The 3-tensor case becomes significantly more complicated and we only provide explicit partition functions for $N = 2$ where we find

$$Z_2^{(3)}(x) = \frac{1 - x^4 + x^8}{(1-x^2)(1-x^4)^4(1-x^6)} \quad (6.24)$$

Expanding in x gives

$$Z_2^{(3)}(x) = 1 + x^2 + 4x^4 + 5x^6 + 12x^8 + 15x^{10} + \dots \quad (6.25)$$

$$Z_2^{(3)}(x_1, x_2) = \frac{P_{2,50}^{(3)}(x, y)}{Q_{2,50}^{(3)}(x_1, x_2)} \quad (6.26)$$

where $P_{2,50}^{(3)}(x_1, x_2)$ has 847 terms. and

$$Q_{2,50}^{(3)}(x_1, x_2) = \prod_{i=1}^2 (1-x_i^2)(1-x_i^4)^4(1-x_i^6) \prod_{n=1}^5 (1-x_1^{6-n}x_2^n)(1-x_1x_2)^3(1-x_1^2x_2^2)^4(1-x_1x_2^3)^4(1-x_1^3x_2)^4 \quad (6.27)$$

$$Z_2^{(3)}(x; 2) = \frac{P_{2,60}^{(3)}(x; 2)}{(1-x^2)^4(1-x^4)^{12}(1-x^6)^6} \quad (6.28)$$

where the even palindromic polynomial $P_{2,60}^{(3)}(x; 2) = 1 + 18x^4 + 90x^6 + 487x^8 + 1844x^{10} + 6523x^{12} + 18546x^{14} + 46581x^{16} + 100536x^{18} + 192179x^{20} + 321634x^{22} + 480212x^{24} + 635840x^{26} + 753583x^{28} + 795508x^{30} + \dots$ which has the expansion

$$Z_2^{(3)}(x; 2) = 1 + 4x^2 + 40x^4 + 236x^6 + 1500x^8 + 7844x^{10} + 37976x^{12} + 162984x^{14} + \dots \quad (6.29)$$

6.4 Hermitian Matrices with adjoint $U(N)$ action.

For a system of d Hermitian matrices X^a , $a = 1, \dots, d$ the thermal action is

$$S[X] = \int_0^\beta d\tau \operatorname{tr} \left(\frac{1}{2} (\mathcal{D}_\tau X^a)^2 + \frac{1}{2} m^2 (X^a)^2 \right) \quad (6.30)$$

where the covariant derivative is now $\mathcal{D}_\tau = \partial_\tau - i[A, \cdot]$ and the gauge field $A(\tau)$ is an $N \times N$ hermitian matrix acting by commutation. The diagonal $U(1)$ acts trivially so that the gauge group is in fact $SU(N)$ but it is convenient to leave this harmless $U(1)$ in the resulting partition function is given by the zero-point energy $\prod_{a=1}^d x_a^{N^2}$ times the normal ordered Molien-Weyl expression:

$$Z_N(x_1, \dots, x_d) = \frac{1}{N!} \oint \prod_{i=1}^N \frac{dz_i}{2\pi i z_i} \Delta(z) \Delta(z^{-1}) \prod_{a=1}^d \prod_{i=1}^N \prod_{j=1}^N \frac{1}{1 - x_a z_i z_j^{-1}}. \quad (6.31)$$

Again one can evaluate partition functions for small N and d .

Explicitly we find

$$Z_2(x, y) = \frac{1}{1 - xy} \prod_{n=1}^2 \frac{1}{(1 - x^n)(1 - y^n)} \quad (6.32)$$

$$Z_3(x, y) = \frac{1 + x^3 y^3}{(1 - xy)(1 - x^2 y)(1 - xy^2)(1 - x^2 y^2)} \prod_{n=1}^3 \frac{1}{(1 - x^n)(1 - y^n)} \quad (6.33)$$

with similar more complicated expressions for $N = 4, 5$ and 6 where

$$Z_2(x; 2) = \frac{1}{(1 - x)(1 - x^2)^3} \quad (6.34)$$

$$Z_3(x; 2) = \frac{1 + x^4 + x^8}{(1 - x)^2 (1 - x^2)^3 (1 - x^3)^4 (1 - x^6)} \quad (6.35)$$

$$Z_4(x; 2) = \frac{(1 - x^{12})(1 + 2x^5 + x^6 + 2x^7 + 4x^8 + 4x^9 + 4x^{10} + 2x^{11} + x^{12} + 2x^{13} + x^{18})}{(1 - x)^2 (1 - x^2)^3 (1 - x^3)^4 (1 - x^4)^6 (1 - x^6)^3} \quad (6.36)$$

The full two parameter expressions for $Z_N(x; 2)$ for $N = 5, 6$ and 7 can be found in can be found in [46] while only the one parameter expression for $N = 7$ has been evaluated [10].

$$Z_3(x_1, x_2, x_3) = \frac{P_8(x_1, x_2, x_3)}{\prod_{n=1}^3 \prod_{i=1}^3 (1 - x_i^n) \prod_{j>i=1}^3 (1 - x_i x_j)^2 (1 - x_i^2 x_j) (1 - x_i x_j^2)} \quad (6.37)$$

with $P_8 = 1 - x_1x_2 - x_1x_3 - x_2x_3 + x_1^2x_2^2 + \cdots - x_1^8x_2^8x_3^8$ a polynomial of degree 8 in each of the x_i which has 158 terms.

$$Z_3(x; 3) = \frac{1 - x - 2x^2 + 6x^3 + 6x^4 - 9x^5 + x^6 + 17x^7 + x^8 - 9x^9 + 6x^{10} + 6x^{11} - 2x^{12} - x^{13} + x^{14}}{(1-x)^4(1-x^2)^8(1-x^3)^7} \quad (6.38)$$

$$Z_3(x_1, x_2, x_3, x_4) = \frac{P_{3,15}(x_1, x_2, x_3, x_4)}{\prod_{n=1}^3 \prod_{i=1}^4 (1 - x_i^n) \prod_{j>i=1}^4 (1 - x_i x_j)^2 (1 - x_i^2 x_j) (1 - x_i x_j^2)} \quad (6.39)$$

with $P_{3,15}(x; 4) = 1 - x_1x_2 - \cdots + x_1^{15}x_2^{15}x_3^{15}x_4^{15}$ a degree 8 polynomial in x_i of degree 15 with a total of 16106 terms.

$$Z_3(x; 4) = \frac{P_{3,24}(x; 4)}{(1-x)^6(1-x^2)^{12}(1-x^3)^{10}} \quad (6.40)$$

$P_{3,24}(x; 4) = g_{3,11}(x; 4) - 76x^{12} + g_{3,11}(\frac{1}{x}; 4)x^{24}$ where $g_{3,11}(x; 4) = 1 - 2x - x^2 + 18x^3 + 6x^4 - 30x^5 + 75x^6 + 150x^7 - 30x^8 + 30x^9 + 401x^{10} + 238x^{11}$.

6.5 The Adjoint Matrix system with $d = 2$ and the $U(1)$ -Charge-0 Sector

A system of pairs of Hermitian matrices X, Y transforming under the adjoint action of $U(N)$ can be used to define a complex $\Phi = X + iY$ which transforms in the adjoint. This system can be restricted to the charge neutral sector by imposing an additional $U(1)$ gauge invariance with an additional $U(1)$ gaugefield so that $\Phi \rightarrow e^{i\theta(\tau)}\Phi$ and $\bar{\Phi} \rightarrow e^{-i\theta(\tau)}\bar{\Phi}$. The covariant derivative in (6.30) then involves an additional $U(1)$ gauge field and the path integral includes integration over this field.

The relevant Molien-Weyl result can then be obtained from the more general complex case given in [6] or equivalently from the Hermitian case by replacing x with zx and in the first determinant and y by x/z thereby including the further integral over the additional z corresponding to the $U(1)$.

In the 2-matrix case where the two matrices transform under the adjoint representation of $U(N)$ we then have

$$Z_N^0(x_1, \dots, x_d) = \oint \frac{dz}{2\pi iz} \frac{1}{N!} \oint \prod_{i=1}^N \frac{dz_i}{2\pi iz_i} \Delta(z) \Delta(z^{-1}) \prod_{i=1}^N \prod_{j=1}^N \frac{1}{1 - zxz_i z_j^{-1}} \frac{1}{1 - z^{-1}xz_i z_j^{-1}} \quad (6.41)$$

These expressions can be evaluated using the known small N results and one finds

$$Z_2^0(x) = \frac{1 + x^4}{(1 - x^2)^2(1 - x^4)^2} \quad (6.42)$$

$$Z_3^0(x) = \frac{1 + 3x^4 + 6x^6 + 9x^8 + 6x^{10} + 12x^{12} + 6x^{14} + 9x^{16} + 6x^{18} + 3x^{20} + x^{24}}{(1 - x^2)^2(1 - x^4)^3(1 - x^6)^3(1 - x^8)} \quad (6.43)$$

$$Z_4^0(x) = \frac{P_{72}^0(x)}{(1-x^2)^2(1-x^4)^3(1-x^6)^4(1-x^8)^4(1-x^{10})^2(1-x^{12})} \quad (6.44)$$

where $P_{72}^0(x)$ is a 36th order palindromic polynomial in x^2 . The denominator order minus the numerator order is $2N^2$ as required from our earlier arguments which require

$$Z_N^0\left(\frac{1}{x}\right) = (-1)^N x^{2N^s} Z^0(x). \quad (6.45)$$

The universal large N low temperature expression for the charge-zero partition function can be obtained from the known expression [50, 76] (8.5) for this limit in the two matrix model and is given by

$$Z_\infty^0(x) = \oint \frac{dz}{2\pi iz} \prod_{n=1}^{\infty} \frac{1}{1 - (z^n + z^{-n})x^n} = \int \frac{d\theta}{2\pi} \prod_{n=1}^{\infty} \frac{1}{1 - 2\cos(n\theta)x^n} \quad (6.46)$$

This expression is well approximated by the first term in the product and on doing the integral one finds

$$Z_\infty^0(x) \simeq \frac{1}{\phi(\frac{1}{2})} \frac{1}{\sqrt{1-4x^2}} \quad (6.47)$$

with $\phi(x) = (x, x)_\infty$ the Euler function and $(a, q)_\infty$ is the q-Pochhammer symbol. This latter expression reproduces the asymptotic counting of charge-zero states as found in [52].

7 High Temperature Limits from path integrals

In the high temperature limit the thermal circle in (6.1) and (6.30) approaches zero circumference and all of the non-zero Matsubara frequencies are driven to up to infinity and decouple. The result is the reduction to a zero dimensional model.

At limiting high temperature (6.1) and (6.30) give classical tensor and matrix models with two terms in their potentials. The first comes from the gauge field interacting with the field Ψ and the second comes from the potential itself. For the finite group case one only has the potential so the scaling at high temperature comes from scaling the temperature dependence and one gets

$$Z_N^{(s)}(x; d) \sim \frac{1}{(m\beta)^{2dN^s}} = \frac{1}{(1-x)^{2dN^s}} \quad (7.1)$$

while the adjoint matrix models with discrete gauge group give $Z_N(x; d) \sim (1-x)^{dN^2}$.

The key point here is that in the high temperature limit only the constant τ independent mode survives. In continuous group case the gauged case the gauge field removes degrees of freedom due to the constraint it implements.

7.1 Matrix Models under Adjoint Action of $U(N)$

For multi-matrix quantum mechanical models (6.30) with d matrices and $d > 1$ the generic counting follows from the Euclidean path integral by first dimensional reduction to time independent model at large N . The reduced path integral is

$$Z_N(x; d) \sim \int [dX][dA] e^{\frac{1}{2}\text{tr}([A, X^a]^2) - \frac{1}{2}\beta^2 m^2 \text{tr}((X^a)^2)} \quad (7.2)$$

where the only temperature dependence is as shown. Then rescaling $X^a = (m\beta)^{-1}\bar{X}^a$ and $A = (m\beta)\bar{A}$ all the temperature dependence is extracted to an overall scale so that asymptotically we have

$$Z_N(x; d) \sim (m\beta)^{(d-1)N^2+1} \int [dX][dA] e^{\frac{1}{2}\text{tr}([\bar{A}, \bar{X}^a]^2) - \frac{1}{2}\text{tr}((\bar{X}^a)^2)} \sim \frac{1}{(1-x)^{(d-1)N^2+1}} \quad (7.3)$$

in agreement with known exact expressions at small N and $d > 1$.

The case of $d = 1$ is special since a single Hermitian matrix gauged under the adjoint action of $U(N)$ can be diagonalized to its eigenvalues which are invariants. The residual phases of the Cartan leave the diagonal matrix invariant and form its stability group. The counting is therefore $N^{N^2-(N^2-N)}$ and the asymptotic behaviour is

$$Z_N(x) \sim \frac{1}{(1-x)^N} \quad (7.4)$$

for two matrices these phases act as $Y_{ij} \rightarrow e^{i(\theta_i - \theta_j)} X_{ij}$ so we can use these phases to remove N of the off diagonal phases of the matrix removing $N - 1$ degrees of freedom. For a third or more matrices there is no freedom to further gauge fix. Hence the counting for $d > 1$ Hermitian matrices can be understood as

$$Z_N(x, d) \sim \frac{1}{(1-x)^{N+(N^2-(N-1))+(d-2)N^2}} = \frac{1}{(1-x)^{dN^2-(N^2-1)}} \quad (7.5)$$

in agreement with the path integral scaling argument. Here dN^2 came from rescaling the d -Hermitian matrices and the $N^2 - 1$ came from rescaling the generators of $U(N)$ for which only $SU(N)$ contributed since the overall $U(1)$ phase cancels due to the adjoint action of the gauge group on the matrices.

For the zero charge sector the additional integration over the $U(1)$ removes an additional phase and the singularity near $x = 1$ gives

$$Z_N^0(x) \sim (1-x)^{-N^2}. \quad (7.6)$$

7.2 Tensor Models

We now consider the tensor models in more detail. Once the high temperature dimensional reduction is performed the resulting path integral, with any temperature dependence removed from the measure, becomes a pure tensor potential model i.e.

$$Z_N^{(3)}(x, d) \sim \int \prod_{k=1}^s [dA^k] \prod_{a=1}^d [d\Psi^a] [d\bar{\Psi}^a] e^{-\sum_{a=1}^d \left(|(A_{i_1 i'_1}^{(1)} + \dots A_{i_s i'_s}^{(s)}) \Psi_{i'_1 \dots i'_s}^a|^2 + \beta^2 m^2 |\Psi_{i_1, \dots, i_s}^a|^2 \right)} \quad (7.7)$$

where the only integration is over the constant modes and the gauge fields. We can extract the temperature and mass dependence from this by rescaling the fields $\Psi_{i,j,k}^a \rightarrow (\beta m_a)^{-1} \Psi_{ijk}^a$ this induces temperature dependence in the gauge field first term which can be cancelled by rescaling $A_a \rightarrow (\beta m) A_a$. We should remember that there is only a single $U(1)$ gauge field. The resulting integration over the tensor and gauge fields has no temperature or mass dependence and is a pure number hence the asymptotic form of the partition function is given by

$$Z_N^{(s)}(x; d) \sim (\beta m)^{s(N^2-1)+1-2dN^s} \sim \frac{1}{(1-x)^{2dN^s-s(N^2-1)+1}}. \quad (7.8)$$

a result which agrees with explicit calculations for the both the 2- and 3-tensor special cases we have calculated. This tells us that the total number of degrees of freedom as distinct from the number of original oscillators is given by

$$N_{\text{phys}} = 2dN^s - s(N^2 - 1) + 1 \quad (7.9)$$

This scaling gives the number of degrees of freedom that behave like free oscillators at high temperature. Since our model has no interactions, only constraints from the gauge invariance, which impose singlet conditions, the high temperature scaling counts the total number of degrees of freedom in the system as opposed to the number of oscillators which is larger being $2dN^s$ and can be accessed by the inversion discussed earlier.

Again for a finite group the gauge field drops out at high temperature since there are no Lie algebra valued connections A^s . The high temperature scaling is therefore always $(1-x)^{2dN^s}$ and $N_{\text{phys}} = 2dN^s$ in the complex case (the exponent is dN^s in the real case).

An alternative understanding of two tensors acted on by $U(N) \otimes U(N)$ is to view them as matrices transforming as

$$\Psi_{ij} \rightarrow U_{ii'} W_{jj'} \Psi_{i'j'} = U_{ii'} \Psi_{i'j'} W^T j' j = (U \Psi V^\dagger)_{ij} \text{ with } W_{j,j'} = V_{j,j'}^* \quad (7.10)$$

Under such a transformation the tensor can be brought into singular value form with diagonal real positive semi-definite entries. For a single tensor these form the N invariants of the system. The stability subgroup that leaves the singular values invariant is the set of the diagonal $U(1)$'s. If there is a second tensor Φ_{ij} we can use the residual action to

remove N of its complex phases but for a 3rd tensor there is no further freedom. For d 2-tensors one can therefore understand the counting for $d > 1$ as

$$Z_N^{(2)}(x; d) \sim \frac{1}{(1-x)^{N+(2N^2-(N-1))+(d-2)2N^2}} = \frac{1}{(1-x)^{2(d-1)N^2+1}} \quad (7.11)$$

The case of complex vectors requires more special cases and the general result (7.9) only applies for $d \geq N$.

7.2.1 Counting Complex Vector Invariants

A complex vector acted on by $U(N)$ can be rotated to a single real component with a residual $U(N-1)$ symmetry. A second vector can be reduced to two components by rotating the normal to the first vector leaving it with 3 real components. One can proceed brought in this fashion till all the freedom associated with $U(N)$ is exhausted for a system of N complex vectors. There is no additional freedom to remove components from more than N such vectors. The first k vectors then give a total of $1 + 3 + \dots + 2k - 1 = k^2$ degrees of freedom and the counting for general d and $U(N)$ is

$$\begin{aligned} N_{\text{phys}} &= d^2 & d \leq N \\ &= 2Nd - N^2 & d \geq N \end{aligned} \quad (7.12)$$

We therefore have the asymptotic scaling for complex vectors as

$$\begin{aligned} Z_N^{(1)}(x; d) &\sim (1-x)^{d^2} & d \leq N \\ &\sim (1-x)^{2Nd-N^2} & d \geq N. \end{aligned} \quad (7.13)$$

8 Hagedorn transitions in $U(N)$ invariant models and negative SHC in tensor models

In this section, we will present a comparison of the thermodynamic properties of the S_N invariant permutation invariant matrix harmonic oscillator thermodynamics we have described in earlier sections and the thermodynamics of $U(N)$ invariant matrix or tensor harmonic oscillator systems. For concreteness, we will discuss the comparison with three cases:

- (I) the quantum mechanics of the $U(N)$ invariant sector of the quantum mechanics of a hermitian matrix under the influence of a harmonic oscillator potential.
- (II) the $U(N)$ invariant sector of two hermitian matrices under the influence of a harmonic oscillator potential.
- (III) the $U(N) \times U(N) \times U(N)$ invariant sector of the quantum mechanics of a complex 3-index tensor Φ_{ijk} with a harmonic oscillator potential.

In all these systems with the number of invariant states with energy k , denoted $\mathcal{Z}(N, k)$, has a universal form for $k \leq N$:

$$\mathcal{Z}(k, N) = \mathcal{Z}(k, M) \equiv \mathcal{Z}(k, \infty) \quad \text{if } M \geq N \geq k \quad (8.1)$$

We refer to this region of the parameters k, N as the stable region. As discussed earlier, there is similar feature in the GPIMQM, with the minor difference that the threshold is at $N = 2k$:

$$Z(k, N) = Z(k, M) \equiv Z(k, \infty) \quad \text{if } M \geq N \geq 2k \quad (8.2)$$

The universal forms in all these cases define positive integer sequences of numbers counting combinatorial objects, which can be defined without reference to N . In all instances considered in this paper, negative SHC arises from the properties of at large k of the counting functions in the stable limit.

The case (I), the invariant states are polynomials in a matrix oscillator A_{ij}^\dagger which are invariant under $U(N)$. The space of states is isomorphic to the space of polynomials of a hermitian matrix invariant under $U(N)$. The vector space of invariants is spanned by traces of the matrix and products of traces (i.e. multi-traces). For a fixed degree k , the number of linearly independent multi-traces is the number of partitions of k , a number which is independent of N . This number grows as $e^{\sqrt{k}}$. The canonical partition function converges for all finite temperatures since $e^{-\beta k + \sqrt{k}}$ vanishes rapidly at large k , for all finite β . This thermodynamics has been discussed in [17] in connection with toy models of AdS/CFT. There is no Hagedorn phase transition in the large N limit. When $k > N$, there are finite N relations between the traces which allow for example the expression of $\text{tr} X^{N+1}$ as a polynomial involving products of lower traces.

The quantisation of the complex harmonic oscillator and gauged complex harmonic oscillator has been discussed in the AdS/CFT context in [16, 55]. There is an equivalent free fermion description of these systems which plays an important role in the dual space of half-BPS supergravity solution [56]. Aspects of the fermion description are discussed in [16, 17, 55, 57]. Information theoretic perspectives on the gravitational thermodynamics for AdS/CFT have been developed using this toy model [58, 59].

The case (II) is a 2-matrix generalisation of (I). The 2-matrix harmonic oscillator is described by a quantum mechanical Lagrangian for two hermitian matrices X, Y with a standard kinetic term and quadratic potential proportional to $\text{tr} X^2 + \text{tr} Y^2$. An identical counting problem arises for the holomorphic sector of a model with two complex matrices which is relevant to the quarter BPS sector $N = 4$ SYM (see [50, 51]). The polynomial functions invariant under unitary transformations $X \rightarrow UXU^\dagger, Y \rightarrow UYU^\dagger$ can be organised according to the degrees (k_1, k_2) in the two matrices. For fixed (k_1, k_2) invariant functions include traces with k_1 copies of X and k_2 copies of Y . This is a counting of necklaces with beads of two colours. The general invariant polynomials at degrees (k_1, k_2) include multi-traces. Let $\mathcal{Z}(k_1, k_2; N)$ be the dimension of the space of invariant

polynomials of degrees (k_1, k_2) for matrices of size N . This counting has a stable form for $k_1 + k_2 \leq N$, i.e. there is a function $\mathcal{Z}(k_1, k_2)$ independent of N such that

$$\mathcal{Z}(k_1, k_2) = \mathcal{Z}(k_1, k_2; N) \text{ for all } N \geq (k_1 + k_2) \quad (8.3)$$

The generating function $\mathcal{Z}(x, y)$ defined as

$$\mathcal{Z}(x, y) = \sum_{k_1, k_2=0}^{\infty} \mathcal{Z}(k_1, k_2) x^{k_1} y^{k_2} \quad (8.4)$$

was shown in [50, 76] to be

$$\mathcal{Z}(x, y) = \prod_{i=1}^{\infty} \frac{1}{(1 - x^i - y^i)} \quad (8.5)$$

The uncolored specialisation of this function $\mathcal{Z}(k) = \sum_{k_1=0}^k \mathcal{Z}(k_1, k - k_1)$ has a generating function

$$\mathcal{Z}(x) = \sum_k \mathcal{Z}(k) x^k = \prod_{i=1}^{\infty} \frac{1}{(1 - 2x^i)} \quad (8.6)$$

From the singularity of the $i = 1$ term in the generating function, it is deduced that there is a Hagedorn transition at $x = e^{-\beta} = 1/2$, i.e. $\beta = \log 2$ [8]. The asymptotic form of the counting $\mathcal{Z}(k)$ has the form $\mathcal{Z}(k) \sim 2^k$. Another interesting asymptotic formula which we will turn to in section 9.2 gives $\mathcal{Z}(r, r) \sim \frac{4^r}{\sqrt{r}}$ [52].

In case (III) we have the invariant theory problem of describing for a complex tensor Φ_{ijk} , with $1 \leq i, j, k \leq N$, the problem of counting invariant functions constructed from k copies of Φ and k copies of $\bar{\Phi}$. This problem also has applications in zero-dimensional tensor integration models. Key initial references are [36][37] while recent overviews of the subject are in [60][61]. A detailed treatment of the counting of the tensor invariants using permutation methods was developed in [38] (see also [62, 64, 63]). The counting function $\mathcal{Z}(n, N)$ has a stable form $\mathcal{Z}(n)$ which is valid for all N obeying $N \geq n$. The universal form counts bi-partite ribbon graphs with n edges and any number of nodes and can also be expressed as a sum of squares of Kronecker coefficients (i.e. Clebsch-Gordan multiplicities for symmetric groups). The tensor counting function was recognised to have an asymptotic growth as $n!$ and this was interpreted in terms of Hagedorn temperature vanishing at large N . Indeed in the infinite N limit, $n!e^{-\beta n}$ grows as $n \rightarrow \infty$ for all finite β . This means that the generating function of invariants in the stable limit $\mathcal{Z}(x) = \sum \mathcal{Z}(n) x^n$ has a vanishing radius of convergence. The all-orders asymptotic formula for $\mathcal{Z}(n)$ was developed in [39].

In the present case of the permutation invariant harmonic oscillator, as we have argued in section 3, there is also a very rapid factorial growth of degeneracies and this is

responsible for the negative specific heat capacity on the low-temperature side of a finite N cross-over transition. This naturally raises the question of whether the tensor model also shows negative specific heat capacity in the micro-canonical ensemble, as we found for the GPIMQM in section 4. In the next sub-section, we will find computational evidence for the negative SHC and will argue, using the results on the high-temperature scaling of the partition function from section 7, that the 3-index tensor harmonic oscillator has the same thermodynamic features as the GPIMQM.

8.1 3-index complex tensor model : Phase structure and computational evidence.

In this section we will consider the quantum mechanics of the a complex 3-index tensor variable with harmonic oscillator potential and gauged $U(N)$ symmetry. The complex tensor Φ_{ijk} transforms in the $V_N \otimes V_N \otimes V_N$ representation of $U(N)$, where V_N is the fundamental. The action and path integral of the gauged quantum mechanics were described in section 6 and the high temperature behaviour of the canonical partition function was derived in 7. As discussed at the beginning of this section, the stable limit of the counting $\mathcal{Z}(n)$ valid when $n \leq N$ has a large n limit which goes like $n!$. This leads directly to a negative SHC in the micro-canonical ensemble. The high temperature behaviour of the canonical partition function is just that of $(2N^3 - 3N^2 + 2)$ harmonic oscillators, this has positive SHC. We expect therefore a turn-over from negative SHC to positive SHC in the micro-canonical ensemble with a breakdown of the equivalence between the canonical and micro-canonical ensemble at low temperatures, all features we have seen in the partition functions of the GPIMQM. In this section, we provide evidence for this picture by using known group-theoretic formulae for $\mathcal{Z}(n, N)$ and demonstrating the turnover from negative SHC to positive SHC for $N = 3$ and $N = 4$.

For energy n , and gauge group $U(N)$, the dimension of the space of invariant states is

$$\mathcal{Z}(n, N) = \sum_{\substack{R_1, R_2, R_3 \vdash n \\ l(R_i) \leq N}} C(R_1, R_2, R_3)^2 \quad (8.7)$$

where $C(R_1, R_2, R_3)$ is the Kronecker coefficient, i.e. the multiplicity of the trivial representation in the tensor product $V_{R_1} \otimes V_{R_2} \otimes V_{R_3}$ of three irreducible representations R_1, R_2, R_3 of S_n .

The computation of the Kronecker coefficients is conveniently done in SAGE [65] using Schur symmetric functions [66]. The short code needed to produce the sums in 8.7 is displayed below:

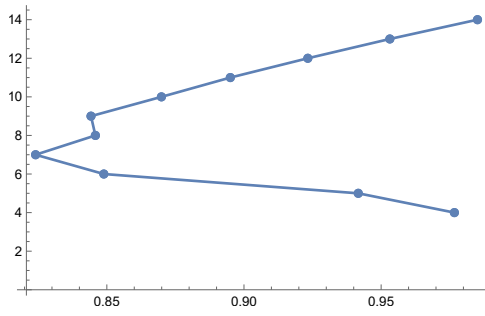


Figure 18: Micro-canonical energy versus temperature for 3-index tensor at $N = 3$ with k equals 3 to 13 using the symmetric D_{sym} discrete derivative

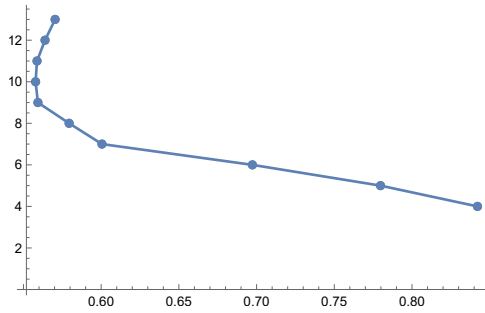


Figure 19: Micro-canonical energy versus temperature for 3-index tensor $N = 4$ with k equals 3 to 12 using the symmetric D_{sym} discrete derivative. Note the curve turns around, i.e. SHC become positive at higher energy.

```
s = SymmetricFunctions(QQ).s()
def Z (n , N ) :
    L = len ( Partitions(n).list() )
    S = 0
    P = Partitions(n).list()
    for i in range(L):
        for j in range (L):
            for k in range (L):
                if len( Partitions(n).list()[i]) < N+1 :
                    if len( Partitions(n).list()[j] ) < N+1 :
                        if len( Partitions(n).list()[k] ) < N+1 :
                            S = S + (s(P[i]).itensor(s(P[j])).scalar ( s( P[k] ) ) )^2
    return S
```

Following this, producing the output for fixed N is done by one-line commands. Going to high n becomes expensive in memory. The computations for $N = 2, 3$ for n up to 11 and 14 respectively are illustrated below

```
[In] [ Z ( i , 2 ) for i in range (12)]
[Out] [1, 1, 4, 5, 12, 15, 30, 37, 65, 80, 128, 156]
[In] [ Z ( i +1 , 3 ) for i in range (14) ]
[Out] [ 1, 4, 11, 31, 92, 327, 1042, 3479, 11136, 34669, 104038, 302494, 848113, 2303667 ]
```

The data $\mathcal{Z}(n, N)$ is copied to Mathematica and used to plot the micro-canonical energy n versus the micro-canonical temperature. The cases $N = 3, 4$ are shown in Figures 18 and 19. They demonstrate the turn-over from negative SHC to positive SHC. In the GPIMQM case, with the more explicit formula (2.11) in hand we were able to

demonstrate this behaviour for N up to 40. Producing the data at higher N and providing detailed evidence that this system is, as argued here, in the same universality class as the GPIMQM is an interesting challenge.

9 Negative SHCs in matrix quantum mechanical models and AdS/CFT

We have seen in section 4 and 8 that super-exponential dependence of the degeneracies $\Omega(k)$ on the non-negative integer energies k leads to negative specific heat capacity in the micro-canonical ensemble. These sequences have an interpretation in terms of different graph counting problems and arise as asymptotic forms in the limit $N \gg k \gg 1$. When we go beyond this regime, and consider k comparable to or larger than N , we get finite N corrections which become significant at sufficiently high k . In the GPIMQM case, we gave computational evidence that this happens at $k \sim \frac{N \log N}{2}$. In this section we will look, in some generality, at different k dependences which lead to negative SHC and discuss these in connection with gauge/gravity duality and black holes, while putting this discussion in the context of other literature on negative SHC in statistical physics.

In section 9.1 we describe classes of super-exponential as well sub-exponential degeneracies which lead to negative specific heat capacities. The key condition is the failure of concavity of $S(k)$, which has been discussed in the context of equivalence/in-equivalence of the micro- and macro-canonical ensembles [44]. An important feature of the GPIMQM is that there is a simple transition between negative SHC and positive SHC in the micro-canonical ensemble, where the transition region occurs on scales of order $x \sim \frac{\log N}{N}$. This behaviour is particularly interesting in the context of AdS5/CFT4, notably the duality between $N = 4$ SYM with $U(N)$ gauge group and string theory on $AdS_5 \times S^5$, where the bulk AdS contains large black holes with positive SHC and small black holes with negative SHC [67, 4]. Of course the GPIMQM employs S_N gauge symmetry, unlike the CFT4. We have also given evidence for similar negative SHC to positive SHC transition in large N systems in the context of $U(N)$ gauge symmetry, in the presence of tensor degrees of freedom. The entropy of small black holes in AdS raises the question of getting negative SHC in multi-matrix systems of the kind that appear in the $N = 4$ SYM. We discuss this for the charge zero complex matrix model in section 9.2. In section 9.3 we discuss an example using multi-matrix counting of $U(N)$ invariants where the number of matrices is taken to scale with the energy. It is useful to put the negative SHCs of GPIMQM in the context of wider discussions of this phenomenon in gravitational systems and generally in statistical physics. We make contact with this wider literature in section 9.3.

Finally, as a point of mathematical interest, the discussion of large N GPIMQM along with matrix/tensor models with S_N or $U(N)$ symmetry has led us to consider a variety of positive integer number sequences having combinatorial interpretations alongside their finite N regularisations offered by natural matrix/tensor systems. We expect that the

purely mathematical study of integer sequences $\Omega(k)$ can be enriched by thermodynamic considerations, particularly (but perhaps even more generally) where they arise as stable limits of matrix/tensor systems having a parameter N , of the kind we have studied in some generality in this paper. As a modest step to indicate the potential of this direction, we present Appendix C where we give an interpretation of the convergence of number sequences and associated sequences of successive ratios in terms of micro-canonical temperatures and specific heat capacities associated with the number sequence.

9.1 Super-exponential and sub-exponential growths of combinatorial sequences and negative specific heat capacities

We start by describing some simple functional forms of degeneracies $\Omega(k)$ associated with positive and negative specific heat capacities.

Example 1: Super-exponential growth - power-correction to linear entropy and negative SHC

Consider $\Omega(k) = e^{ak^b}$ for constants a and b , with $a > 0$. The integer k is identified as energy. It is easy to show that if $b > 1$ then the specific heat capacity is negative. The entropy is

$$S(k) = \log \Omega(k) = ak^b \quad (9.1)$$

The micro-canonical inverse temperature

$$\begin{aligned} \beta_{\text{micro}} &= T_{\text{micro}}^{-1} = \frac{\partial S(k)}{\partial k} = abk^{b-1} \\ T_{\text{micro}} &= a^{-1}b^{-1}k^{1-b} \\ \frac{\partial T_{\text{micro}}}{\partial k} &= a^{-1}b^{-1}(1-b)k^{-b} \\ C_{\text{sh;micro}} &= \left(\frac{\partial T_{\text{micro}}}{\partial k} \right)^{-1} = \frac{ab}{(1-b)}k^b \end{aligned} \quad (9.2)$$

It is clear that for $a > 0$, and $b > 1$, we have negative SHC. The range $a > 0, b > 1$ corresponds to super-exponential degeneracies, $b < 1$ is sub-exponential.

Example 2: Weakly super-exponential and negative SHC

We consider

$$\Omega(k) = e^{ak(\log k)^b} \quad (9.3)$$

$$\beta_{\text{micro}}(k) = ab \log^{b-1}(k) + a \log^b(k)$$

$$\frac{\partial \beta_{\text{micro}}}{\partial k} = abk^{-1} \log^{b-2}(k)(b + \log(k) - 1) \quad (9.4)$$

This give a micro-canonical heat capacity

$$C_{\text{hc}}(k) = -\beta_{\text{micro}}(k)^2 \left(\frac{\partial \beta_{\text{micro}}}{\partial k} \right)^{-1} = -\frac{ak \log^b(k)(b + \log(k))^2}{b(b + \log(k) - 1)} \quad (9.5)$$

for large positive integer $k \gg 1$ and b order 1, we have

$$C_{\text{hc}}(k) \sim -\frac{ak}{b} \log^{b+1}(k) \quad (9.6)$$

We are interested in large positive integer k . In this regime it is evident that $C_{\text{sh}}(k)$ is negative for the super-exponential degeneracies with $a > 0, b > 0$, while it is positive for near-exponential but sub-exponential case $a > 0, b < 0$.

Along similar lines, for

$$\Omega(k) = e^{ak(\log(\log k))^b} \quad (9.7)$$

the micro-SHC is

$$C_{\text{hc};\text{micro}}(k) = -\frac{ak \log^b(\log(k))(b + \log(k) \log(\log(k)))^2}{b(b + (\log(k) - 1) \log(\log(k)) - 1)} \quad (9.8)$$

and at large k ,

$$C_{\text{hc};\text{micro}}(k) \sim \frac{-ak}{b} (\log(\log(k)))^{b+1} \log(k) \quad (9.9)$$

At large integer k , we get negative SHC for the super-exponential growths $a > 0, b > 0$ while for the near-exponential but sub-exponential growths, we have positive SHC.

Example 3: Power-law corrections to large k exponential growth

Consider for $d > 1$, the degeneracies which have near-exponential growth as a function of k

$$\Omega(k) = d^k k^a = e^{k \log d + a \log k} \quad (9.10)$$

The micro-canonical $\beta_{\text{micro}}(k)$ is

$$\beta_{\text{micro}}(k) = \log d + \frac{a}{k} \quad (9.11)$$

In the large k limit, which is relevant to convergence of the partition function

$$\beta_{\text{micro}}(k \rightarrow \infty) = \log d \quad (9.12)$$

The derivative

$$\frac{\partial \beta_{\text{micro}}(k)}{k} = -\frac{a}{k^2} \quad (9.13)$$

The micro-canonical heat capacity $c_{\text{hc}; \text{micro}}(k)$ is

$$C_{\text{hc}; \text{micro}}(k) = \frac{k^2}{a} (\log d + \frac{a}{k})^2 \quad (9.14)$$

In the large k limit,

$$\begin{aligned} C_{\text{hc}; \text{micro}}(k \rightarrow \infty) &= \frac{k^2 \log d}{a} \\ &< 0 \text{ for } a < 0 \\ &> 0 \text{ for } a > 0 \end{aligned} \quad (9.15)$$

This has the interesting consequence that these are simple functional forms of degeneracies which can be sub-exponential, while having negative SHC,

$$C_{\text{hc}; \text{micro}}(k) < 0 \quad \text{for } \Omega(k) \sim d^k k^a \text{ with } a < 0 \quad (9.16)$$

and super-exponential while having positive SHC

$$C_{\text{hc}; \text{micro}}(k) > 0 \quad \text{for } \Omega(k) \sim d^k k^a \text{ with } a > 0 \quad (9.17)$$

This is to be contrasted with the examples 1 and 2, where the super-exponential forms have positive SHC and the sub-exponential forms have negative SHC.

9.2 Negative SHCs from zero-charge sector of complex matrix quantum mechanics and AdS/CFT

There is an interesting instance of the Example 3 above, in the case of the 2-matrix model where the asymptotics of 2-matrix invariants was derived in [52] using multi-variate asymptotic methods of [68]. It is interesting to express the result for the case of complex matrices Z, Z^\dagger with r copies of Z and s copies of Z^\dagger , $N \gg r, s \gg 1$. The case $r = s$ can be interpreted as a zero charge non-BPS system which, for large enough r , may be interpreted in terms of brane/anti-brane systems (see e.g. [69]). Specialising the asymptotics to $r = s$, the coefficients take the form [52]

$$\Omega(r) = a_{rr} \sim \frac{G(\frac{1}{2}, \frac{1}{2})}{\sqrt{\pi}} \frac{4^r}{\sqrt{r}} \quad (9.18)$$

where

$$G(\frac{1}{2}, \frac{1}{2}) = \prod_{i=2}^{\infty} (1 - 2^{-i+1}) \quad (9.19)$$

is an inverse QPochhammer function $(a, q)_n$ specialised to $a = 1/2, q = 1/2, n = \infty$. This is an instance of the discussion in Example 3 above with $d = 4, a = \frac{-1}{2}$ (the overall constant $\frac{G(1/2, 1/2)}{\sqrt{\pi}}$ does not affect the temperature or heat capacity). In the large N system at hand, the thermodynamic quantities which are finite in the $N \rightarrow \infty$ limit are obtained by dividing with N^2 . The SHC thus defined

$$C_{\text{sh;micro}} = \frac{C_{\text{hc;micro}}}{N^2} \quad (9.20)$$

approaches 0 from the negative side on the low energy branch of the $E - T$ curves as $N \rightarrow \infty$. The heat capacity becomes infinite at the low temperature end of the $E - T$ curve. Based on the similarities with the 2-matrix quantum mechanics without zero charge condition [49] we expect that the energy at this transition scales like N^2 and for energies sufficiently close to this threshold the specific heat capacity will be finite and negative.

Using the asymptotic form of the partition function in the canonical partition function we have the sum

$$\sum_r \frac{e^{2r \log 2 - \beta r}}{\sqrt{r}} \quad (9.21)$$

which diverges at $\beta = 2 \log 2 \equiv \beta_H$ due to the near-exponential growth of degeneracies at large r . This is thus a Hagedorn transition similar to the 2-matrix harmonic oscillator. The heat capacity at finite temperatures will be positive as required by the standard general argument reviewed in section 3. After rescaling by N^2 , the specific heat capacity at fixed temperatures below β_H approaches zero from positive values as N approaches infinity. There is an in-equivalence of ensembles at finite N , which in an appropriate physical sense, tends to zero as $N \rightarrow \infty$.

Nevertheless, as explained above, for a small range of temperatures near the minimum in the micro-canonical ensemble, the SHC is negative at large N . It will be interesting to investigate the bulk interpretation of this negative SHC further in the context of long-range attractive forces which are known to produce negative SHC [70, 44, 71].

We will present computational evidence that there indeed is negative heat capacity in the micro-canonical ensemble which turns to positive heat capacity. The computations are based on the finite N formula for multi-matrix invariants in terms of Littlewood-Richardson coefficients. For polynomial functions of two matrices Z and Z^\dagger , invariant under $Z \rightarrow UZU^\dagger$ and of degree (m, n) in (Z, Z^\dagger) , the dimension of the space of polynomials is

$$\sum_{R \vdash m, S \vdash n} \sum_{\substack{T \vdash (m+n) \\ l(T) \leq N}} (g(R, S, T))^2 \quad (9.22)$$

where R, S, T are Young diagrams with $m, n, (m+n)$ boxes respectively ; $g(R, S, T)$ is the Littlewood-Richardson coefficient for the triple ; and T is restricted to have no more than

N rows. This formula plays a role in the construction of orthogonal restricted Schur bases for multi-matrix operators in free field theory [72, 73, 76]. We expect that this positive heat capacity branch extends to the high temperature regime derived using the quantum mechanical path integral in section 3.3.

Figure 20 gives the micro-canonical energy versus temperature plot for $N = 13$, showing a short positive branch before the near-exponential asymptotic form of the stable degeneracy function sets in. This is followed by a negative heat capacity branch over a range of temperatures which is expected to grow in size with N . This negative SHC branch does not exist for $N \leq 11$, just about appears for $N = 12$ but is clearly visible for $N = 13$. The negative heat capacity branch extends over a larger range of temperatures for $N = 15, 17$ and is expected to extend over an increasing range of temperatures in the large N limit. We expect the negative HC branch to reach a minimum temperature and turn around to a positive SHC branch which connects with the high temperature limit.

The sequence of degeneracies for $N = 13$ is calculated in SAGE using the formula

$$\sum_{R, S \vdash n} \sum_{T \vdash 2n} (g(R, S, T))^2 \quad (9.23)$$

which specialises (9.22) to $m = n$. The output for $n = 1$ to $n = 13$ is

$$\{2, 10, 38, 158, 602, 2382, 9141, 35477, 136790, 529258, 2045921, 7921783, 30675577, 118850945, 460430464, 1783233892, 6901543295, 26683631076\} \quad (9.24)$$

The sequence for $N = 15$ going up to $n = 16$ is

$$\{2, 10, 38, 158, 602, 2382, 9142, 35491, 136921, 530258, 2052698, 7964239, 30925953, 120260841, 468079803, 1823504895\} \quad (9.25)$$

This value of n is not high enough to see the start of the negative SHC branch at $N = 15$.

The SAGE code giving these outputs is shown in Appendix D.

9.3 Negative SHC with super-exponential growth of degeneracies in multi-matrix models

There is a group theoretic formula for counting the $U(N)$ invariant polynomials of degree k in d matrix variables of size N which has been used in the construction of orthogonal bases of gauge invariant operators [9, 50, 74, 75, 76]

$$Z(n, d, N) = \sum_{\substack{R \vdash k \\ l(R) \leq N}} \sum_{\substack{\Lambda \vdash k \\ l(\Lambda) \leq d}} C(R, R, \Lambda) \text{Dim}_{U(d)} \Lambda \quad (9.26)$$

The sum is over Young diagrams R with k boxes, constrained to have no more than N rows, and Young diagrams Λ with k boxes and no more than d rows. $C(R, R, \Lambda)$ is the

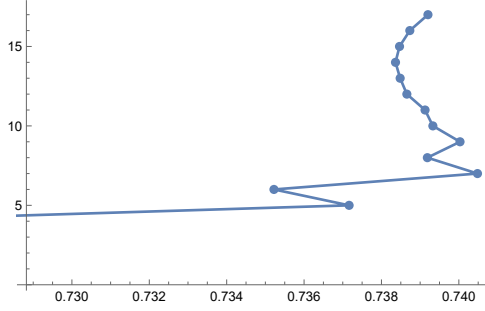


Figure 20: Micro-canonical energy versus temperature for zero charge complex matrix system $N = 13$ with k equals 3 to 18 using the symmetric D_{sym} discrete derivative. Note the curve has a short positive SHC branch, a negative SHC branch (expected to grow in size with N) and a positive SHC branch expected to connect to extend to the high temperature limit.

number of trivial representations of S_k in the decomposition of the tensor product $R \otimes R \otimes \Lambda$ into irreducible representations of the diagonal S_k , i.e. the Kronecker coefficient for the triple of Young diagrams (R, R, Λ) . $\text{Dim}_{U(d)} \Lambda$ is the dimension of the $U(d)$ representation corresponding to Young diagram Λ . The formula simplifies in the case $d, N \geq n$:

$$Z(k, d, N) = Z(k, d) = \sum_{l=0}^k d^l P(k, l) \quad (9.27)$$

$P(k, l)$ is the number of partitions of k with l parts. The leading term is d^k , coming from the partition $[1^k]$.

A simple and surprisingly useful observation is that since $\text{Dim}_{U(d)} \Lambda$ in (9.26) is zero for $l(\Lambda) > d$, we can extend the summation to all partitions Λ of k . This sum over Λ can be done using character orthogonality to simplify the expression

$$\begin{aligned} Z(k, d, N; d \geq k) &= \sum_{\substack{R \vdash k \\ l(R) \leq N}} \sum_{\Lambda \vdash k} C(R, R, \Lambda) \text{Dim}_{U(d)} \Lambda \\ &= \frac{1}{(k!)^2} \sum_{\substack{R \vdash k \\ l(R) \leq N}} \sum_{\Lambda \vdash k} \sum_{\sigma} \chi^R(\sigma) \chi^R(\sigma) \chi^\Lambda(\sigma) \sum_{\tau \in S_k} \chi^\Lambda(\tau) d^{C_\tau} \\ &= \sum_{\substack{R \vdash k \\ l(R) \leq N}} \sum_{\Lambda \vdash k} \sum_{p \vdash k} \sum_{q \vdash k} \frac{1}{\text{Sym} p} \frac{1}{\text{Sym} q} \chi_p^R \chi_p^R \sum_{\Lambda} \chi_p^\Lambda \chi_q^\Lambda d^{C_q} \end{aligned} \quad (9.28)$$

We used the expression for the Kronecker coefficient as a sum of characters. In the last line, we have converted the sum over σ to a sum over partitions p and the sum over τ to a sum over partitions q . χ_p^R is the character of a permutation σ_p in conjugacy class p for the

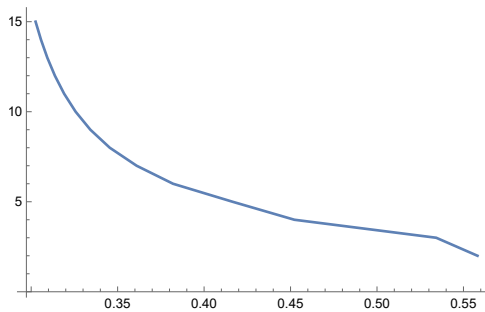


Figure 21: Micro-canonical energy versus temperature for $(d = n)$ -scaled multi-matrix model with $N = 4$ and n between 2 and 15 : negative slope evidences the negative SHC

irreducible representation Λ . We can do the sum over Λ using character orthogonality.

$$\sum_{\Lambda} \chi^{\Lambda}(\sigma_p) \chi^{\Lambda}(\sigma_q) = \delta_{p,q} \text{ Sym } p \quad (9.29)$$

Therefore

$$Z(n, d, N) = \sum_{p \vdash k} \frac{d^{C_p}}{\text{Sym } p} \sum_{\substack{R \vdash n \\ l(R) \leq N}} \chi_p^R \chi_p^R \quad (9.30)$$

This formula is conveniently coded in SAGE (see Appendix E). A closely related formula is discussed in [77] in the context of unitary matrix integrals.

The formulae here allow us to investigate an interesting limit of the multi-matrix counting, namely one where $d = k$, i.e we are taking the number of matrices to increase as the energy increases. This can be heuristically motivated by the counting of free field operators in $N = 4$ SYM : at higher energies, i.e. dimensions of local operators, we have more matrix fields, e.g. derivatives of the six hermitian matrix scalars. The present counting (9.26) treats all the d matrices as having dimension 1 so is by no means a precise reflection of the free field $\mathcal{N} = 4$ counting, but can be viewed as a tractable toy model for investigating the effects of increasing the number of matrices as the dimension increases - which has not yet been done in attempts to explore how the physics of small black holes arises from multi-matrix combinatorics in $\mathcal{N} = 4$ SYM. The leading term in (9.27) $d^k \sim k^k$ has the negative SHC property. A somewhat exotic scaling of d with k , namely $d \sim e^{k^{1/7}}$ produces, from d^k an entropy $S(k) = \log \Omega(k) \sim k^{8/7}$ which matches that of ten-dimensional Schwarzschild black holes, which is a natural scaling to look for in connection with small black holes in $AdS_5 \times S^5$ (see an earlier discussion of an attempt towards this scaling from a different point of view in [78] and more recent attempts from a similar perspective [53][54] [82]). We leave a more systematic investigation of negative SHC in the context well-motivated multi-matrix constructions emulating the physics of small black holes in $AdS_5 \times S^5$ for the future. Understanding the physics of

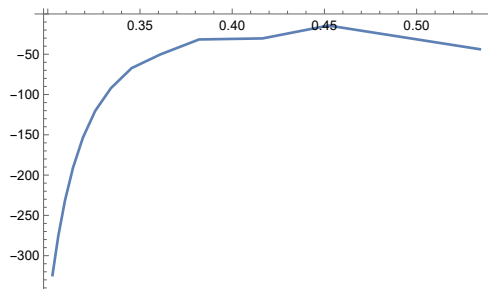


Figure 22: Micro-canonical SHC versus temperature for $(d = n)$ -scaled multi-matrix model with $N = 4$ and n between 2 and 15.

small black holes in $AdS_5 \times S^5$ from the point of view of CFT4 remains a fascinating open problem. The negative specific heat capacities found in the context of tractable group-theoretic counting problems associated with gauge invariants in well defined simple quantum mechanical models of the kind considered here may be expected to be a useful ingredient in this quest.

Another reason for exploring negative SHCs in multi-matrix models with d scaling as n is that novel scalings of d in multi-matrix models are known [79] to reproduce certain aspects of the physics of tensor models, in particular the existence of limits dominated by melonic interactions. We have in section 8 that tensor models display negative SHCs at finite N , so it is natural to explore this feature in multi-matrix models with novel scalings.

10 Summary and Outlook

We have investigated the thermodynamics of the permutation invariant sector of a quantum system of matrix oscillators. The partition function for this invariant sector was realised as a path integral in [6] and the canonical partition function was computed for general matrix size N in [7]. We used the explicit formula for the partition functions to derive an all-orders high-temperature expansion. The breakdown of the high temperature expansion occurs at a scale of order $x \sim \frac{\log N}{N}$. We perform numerical studies of the thermodynamics for a range of values of N typically up to 40 (and up to 70 for some calculations). We find evidence for a sharp transition in the expectation value of the energy in the canonical ensemble, with $x = e^{-1/T}$, at x of order $x_c = \frac{\log N}{N}$. The micro-canonical ensemble reveals that the micro-canonical energy $E = \frac{k}{N^2}$ as a function of temperature has two branches, see Figure 11. In the low energy branch the micro-canonical specific heat capacity (figure 13) is negative while in the high energy branch it is positive. The transition is found numerically to occur at approximately $k \sim \frac{N \log N}{2}$. As

previously discussed, the canonical ensemble always has positive specific heat capacity. Setting the micro-canonical and canonical temperatures equal gives good agreement between the ensembles above the transition region $x \sim \frac{\log N}{N}$ (see Figure 15). We note that the micro-canonical transition always occurs at a lower temperature than the canonical one see Figure 17, but both go to zero at large N , as required by our high temperature result.

By using the path integral formula for multi-matrix and tensor model partition functions, we obtained their high temperature scaling. This gives nice expressions for the total number of invariants N_{phys} in the system (eqn (7.8)) and establishes that the high temperature thermodynamics is that of a free system of N_{phys} oscillators.

Computations of the degeneracies at low energies, with the help of representation theoretic formulae for the micro-canonical data, gives evidence that the features of negative specific heat capacity and ensemble inequivalence also occur in certain multi-matrix and tensor systems. Hence such systems have a low temperature region with negative micro-canonical specific heat and a high temperature positive specific heat. In particular we found that the charge zero sector of the Hermitian two-matrix model (with the two matrices rotating under an additional $U(1)$ or $SO(2)$) again has a Hagedorn type transition at $T_H = \frac{1}{\ln 2}$ but the low temperature approach to this transition is described in eqn (6.46) in contrast to eqn (8.5) for the two matrix model.

We now describe a number of interesting future research avenues arising from this work. We have focused here on the thermodynamics of the simplest gauged permutation invariant quantum mechanical harmonic oscillator system. The quadratic potential is one of eleven linearly independent quadratic functions of the matrix variables, which was described in the context of matrix quantum mechanics in [33]. The canonical partition functions were computed for the general 11-parameter case in [6]. Extending the present investigation, of the thermodynamics to a more detailed analysis of the general 11-parameter case, would give useful perspective on the results here. In particular it would be interesting to further investigate the negative micro-canonical SHC in this setting.

We have found that the quantum mechanical 3-index tensor model with $U(N)$ symmetry has negative micro-canonical SHCs and shown in a general discussion that this is expected from the growth of the degeneracies of its states. Exploring this feature for more general tensor models, for example those with $O(N)$ or $Sp(N)$ gauge groups (see e.g. [80] [81] for investigations in this area and for further references), would be especially interesting.

In our discussion of negative SHC in the zero charge sector of a complex matrix (or equivalently the Hermitian 2-matrix model) we discussed the interpretation in terms of branes and anti-branes. A derivation of this feature directly from brane/anti-brane systems in the bulk of AdS would be fascinating. Existing general discussions, e.g. [70][71], of negative specific heat capacities in connection with long-range interactions are

likely to be useful as ingredients in such a project.

The close qualitative similarity between the phase structure of the thermodynamics of the permutation invariant one-matrix model and the $U(N)$ invariant 3-index tensor model should be explored more quantitatively. The idea of using discrete versions of continuous symmetries as an approximation scheme to study the physics of a system with continuous symmetries has been used in lattice gauge theory (see e.g. [84, 85, 86]). The present case, where the matter content is changed from matrix to tensor while the gauge group is changed from continuous to discrete, is an interesting twist on the idea. Finding further examples of this kind of connection within matrix/tensor systems would give an important perspective on this intriguing similarity.

Acknowledgments

SR is supported by the Science and Technology Facilities Council (STFC) Consolidated Grants ST/P000754/1 “String theory, gauge theory and duality” and ST/T000686/1 “Amplitudes, strings and duality” and a Visiting Professorship at Dublin Institute for Advanced Studies. We thank Joseph Ben Geloun, Brian Dolan, Thomas Fink, Masanori Hanada, Yang-Hui He, Ed Hirst, Chris Hull, Forrest Sheldon, Michael Stephanou, Lewis Sword for discussions related to the subject of this paper.

A Multi-harmonic oscillator and ensemble equivalence

The high temperature limit of the canonical ensemble for the permutation invariant harmonic oscillator in section 3 and for vector, matrix and tensor harmonic oscillator models with unitary gauge invariance are given by some number of decoupled harmonic oscillators. It is useful to review the key formulae for the thermodynamics of M copies of the simple harmonic oscillator.

The canonical partition function is

$$Z(M, x) = \frac{1}{(1-x)^M} \quad (\text{A.1})$$

The thermodynamic quantities in the canonical ensemble are as follows:

$$\begin{aligned} \text{Energy:} \quad U &= x \frac{\partial \log Z}{\partial x} = \frac{Mx}{(1-x)} \\ \text{Heat capacity:} \quad C_{\text{hc}}(x) &= (\log x)^2 x \frac{\partial U}{\partial x} = \frac{Mx \log^2(x)}{(x-1)^2} \\ \text{Entropy:} \quad S &= \log Z - (\log x)U(M, x) = \frac{Mx \log(x)}{x-1} - M \log(1-x) \end{aligned}$$

(A.2)

In the high temperature limit, $T \rightarrow \infty, \beta \rightarrow 0, x \rightarrow 1, C_{\text{hc}}(x) \rightarrow M$.
Solving for x as a function of U

$$x = \frac{U}{(M + U)} \quad (\text{A.3})$$

As an equation for the inverse temperature

$$\beta = \log\left(1 + \frac{M}{U}\right) \quad (\text{A.4})$$

Substituting $x(U)$ in the entropy to get the entropy as a function of U ,

$$S(U) = (M + U) \log(M + U) - M \log M - U \log U \quad (\text{A.5})$$

Getting the specific heat capacity as a function of U

$$C_{\text{hc}}(U) = U \left(1 + \frac{U}{M}\right) \left(\log\left(1 + \frac{M}{U}\right)\right)^2 \quad (\text{A.6})$$

Expanding the canonical partition function

$$Z(M, x) = \sum_{n=0}^{\infty} \Omega(M, n) x^n \quad (\text{A.7})$$

where

$$\Omega(M, k) = \frac{(M + k - 1)!}{(M - 1)!k!} \quad (\text{A.8})$$

We can define the micro-canonical inverse-temperature using the discrete derivative

$$Df(k) = f(k) - f(k - 1) \quad (\text{A.9})$$

to obtain

$$\begin{aligned} \beta_{\text{micro}}(k) &= D \log(\Omega(M, k)) = (\log \Omega(M, k) - \log \Omega(M, k - 1)) \\ &= \log \left(\frac{\Omega(M, k)}{\Omega(M, k - 1)} \right) \end{aligned} \quad (\text{A.10})$$

which simplifies to

$$\beta_{\text{micro}}(k) = \log \left(\frac{(M + k - 1)!}{(M - 1)!k!} \right) = \log \left(1 + \frac{(M - 1)}{k} \right) \quad (\text{A.11})$$

Setting $k \rightarrow U$, i.e. the exact energy of the micro-canonical ensemble to the expectation value of the energy in the canonical ensemble, we get

$$\beta_{\text{micro}}(k(U)) = \log \left(1 + \frac{(M-1)}{U} \right) \quad (\text{A.12})$$

This agrees with (A.4) in the large M limit.

$$\beta_{\text{micro}}(k(U)) \sim \beta(U) \quad \text{Large } M \quad (\text{A.13})$$

The entropy in the micro-ensemble is

$$S_{\text{micro}}(k) = \log \Omega(k) = \log(M+k-1)! - \log(M-1)! - \log k! \quad (\text{A.14})$$

In the large k limit, using Stirling's formula,

$$\begin{aligned} S_{\text{micro}}(k) &\sim (M+k) \log(M+k) - (M+k) - M \log M + M - k \log k + k \\ &= (M+k) \log(M+k) - M \log M - k \log k \end{aligned} \quad (\text{A.15})$$

This agrees with the formula for the entropy as a function of the expectation value of the energy U , upon the identification $k \rightarrow U$. We thus see the use of the large M limit.

To see the matching of the specific heat capacity,

$$C_{\text{hc};\text{micro}}(k) = -\frac{\beta_{\text{micro}}^2(k)}{D\beta_{\text{micro}}(k)} \quad (\text{A.16})$$

When $M \gg 1$,

$$\beta_{\text{micro}}(k) = \log\left(1 + \frac{M}{k}\right) \quad (\text{A.17})$$

The discrete derivative

$$\begin{aligned} D\beta_{\text{micro}}(k) &= \beta_{\text{micro}}(k) - \beta_{\text{micro}}(k-1) \\ &= \log\left(1 + \frac{M}{k}\right) - \log\left(1 + \frac{M}{k-1}\right) \\ &= \log\left(1 + \frac{M}{k}\right) - \log\left(1 + \frac{M}{k(1-1/k)}\right) \\ &\sim \log\left(1 + \frac{M}{k}\right) - \log\left(1 + \frac{M}{k}\left(1 + \frac{1}{k}\right)\right) \end{aligned} \quad (\text{A.18})$$

In the last line, we used $k \gg 1$. This simplifies to

$$\begin{aligned} D\beta_{\text{micro}}(k) &\sim \log\left(1 + \frac{M}{k}\right) - \log\left(1 + \frac{M}{k}\right)\left(1 + \frac{M}{k^2}\left(1 + \frac{M}{k}\right)^{-1}\right) \\ &= -\log\left(1 + \frac{M}{k^2}\left(1 + \frac{M}{k}\right)^{-1}\right) \end{aligned}$$

$$(A.19)$$

Assuming now $\frac{M}{k^2}(1 + \frac{M}{k})^{-1} \ll 1$, we have

$$D\beta_{\text{micro}}(k) = -(\frac{M}{k^2}(1 + \frac{M}{k})^{-1}) \quad (A.20)$$

Note that this is solved by $k \gg M$, but is also solved by weaker conditions such as $k \gg \sqrt{M}, \frac{k}{M}$ Order 1. Then

$$\begin{aligned} C_{\text{hc;micro}}(k) &= \frac{k^2}{M}(1 + \frac{M}{k})(\log(1 + \frac{M}{k}))^2 \\ &= k(1 + \frac{k}{M})(\log(1 + \frac{M}{k}))^2 \end{aligned} \quad (A.21)$$

This agrees with (A.6). The assumptions we made are $k \gg 1, M \gg 1, k^2 \gg M$, i.e. $k \gg \sqrt{M}$. We have not assumed $k \gg M$. If we make that stronger assumption, then

$$C_{\text{hc;micro}} \sim C_{\text{hc;can}} \sim M \quad (A.22)$$

B Proving that the first sub-leading term in the high temperature expansion is from $p = [2, 1^{N-2}]$

We have shown in section 5 that the leading term in the high temperature expansion of (2.15), comes from $p = [1^N]$ with a pole of order N^2 at $x = 1$. The term from $p = [2, 1^{N-2}]$ has a pole of order $N^2 - 2N + 2$. Here we show that all other p lead to poles of lower order.

We will define p_{gen} to be a general partition having multiplicities $p_1, p_2 = q_2 + 1, p_3 \dots, p_K$ for parts $1, 2, a_3, a_4, \dots, a_K$, with $a_K > a_{K-1} > \dots > a_3 \geq 3$ and $N = p_1 + 2p_2 + \sum_{i \in \{3, \dots, K\}} a_i p_i$. We will denote as $p_* = [1^{N-2}, 2] = [1^{p_1+2q_2+a_3p_3+\dots+a_Kp_K}, 2]$ and we will compare to p_{gen} . Thus the key definitions are :

$$\begin{aligned} p_{\text{gen}} &= [1^{p_1}, 2^{q_2+1}, a_3^{p_3}, \dots, a_K^{p_K}] \\ p_* &= [1^{p_1+2q_2+a_3p_3+\dots+a_Kp_K}, 2] \\ \text{Diff}(p_{\text{gen}}, p_*) &= \text{Deg}(p_{\text{gen}}) - \text{Deg}(p_*) \end{aligned} \quad (B.1)$$

We need $q_2 \geq -1$ to ensure that the number of 2-cycles in p_{gen} is non-negative. If $q_2 = -1$, we need $p_1 + a_3p_3 + \dots + a_Kp_K \geq 2$. Denote $S = \{1, 3, \dots, K\}$ and $S' = \{3, \dots, K\}$. Using the formula for the degree of partitions (eqn (5.5)), which determines the degree of the singularity in $\mathcal{Z}(N, x)$ at $x = 1$, we calculate

$$\text{Deg}(p_{\text{gen}}) = 2(q_2 + 1)^2 + \sum_{i \in S} a_i p_i^2 + 2(q_2 + 1) \sum_{j \in S} p_j G(2, a_j) + 2 \sum_{i < j \in S} p_i p_j G(a_i, a_j) \quad (B.2)$$

We also calculate

$$\begin{aligned}
\text{Deg}(p_*) &= 2 + (2q_2 + \sum_{i \in S} a_i p_i)^2 + 2(2q_2 + \sum_{i \in S} a_i p_i) \\
&= 2 + 4q_2^2 + 4q_2 \sum_{i \in S} a_i p_i + \sum_{i \in S} a_i p_i \sum_{j \in S} a_j p_j + 4q_2 + 2 \sum_{i \in S} a_i p_i \\
&= 2 + 4q_2^2 + 4q_2 \sum_{i \in S} a_i p_i + \sum_{i \in S} a_i^2 p_i^2 + 2 \sum_{i < j \in S} p_i p_j a_i a_j + 4q_2 + 2 \sum_{i \in S} a_i p_i
\end{aligned} \tag{B.3}$$

We will show that $\text{Deg}(p_{\text{gen}}) - \text{Deg}(p_*) < 0$ for all p_{gen} as long as $p_{\text{gen}} \neq p_*, p_{\text{gen}} \neq [1^N]$. For the difference

$$\begin{aligned}
\text{Diff}(p_{\text{gen}}, p_*) &= \text{Deg}(p_{\text{gen}}) - \text{Deg}(p_*) \\
&= -2q_2^2 + \sum_{i \in S} a_i p_i^2 + 2(q_2 + 1) \sum_{j \in S} p_j G(2, a_j) + 2 \sum_{i < j \in S} p_i p_j G(a_i, a_j) \\
&\quad - (2q_2 + 2(q_2 + 1)) \sum_{i \in S} a_i p_i - \sum_{i \in S} a_i^2 p_i^2 - \sum_{i < j \in S} 2p_i p_j a_i a_j \\
&= -2q_2^2 - \sum_{i \in S} (a_i^2 - a_i) p_i^2 - 2(q_2 + 1) \sum_{i \in S} (a_i - G(2, a_i)) p_i - 2 \sum_{i < j \in S} p_i p_j (a_i a_j - G(a_i, a_j)) - 2q_2 \sum_{i \in S} a_i p_i
\end{aligned} \tag{B.4}$$

Now we observe the identities

$$\begin{aligned}
a_i - G(2, a_i) &\geq 0 \\
a_i a_j - G(a_i, a_j) &\geq 0
\end{aligned} \tag{B.5}$$

which follow because the GCD of two integers cannot exceed either integer. We also observe

$$a_i^2 - a_i = a_i(a_i - 1) \geq 0 \tag{B.6}$$

with the equality holding for $a_1 = 1$ and the strict inequality holding for a_3, \dots . It is evident that $\text{Diff}(p_{\text{gen}}, p_*) \leq 0$ for $q_2 \geq 0$. We need to show that the only time it is zero is if $q_2 = 0$ and $p_3, \dots = 0$, which ensures that $p_{\text{gen}} = p_*$. Note that $(a_1 - G(2, a_1)) = 1 - G(2, 1) = 0$ and recall $S' = \{3, 4, \dots, K\}$. It is useful at this stage to separate out the contributions from $i = 1$ and $i \in S'$ in the sums over S in (B.4). The difference of degrees is thus expressed as:

$$\begin{aligned}
\text{Diff}(p_{\text{gen}}, p_*) &= -2q_2^2 - \sum_{i \in S'} a_i(a_i - 1)p_i^2 - 2(q_2 + 1) \sum_{i \in S'} (a_i - G(2, a_i)) p_i \\
&\quad - 2p_1 \sum_{j \in S'} p_j(a_j - G(1, a_j)) - 2 \sum_{i < j \in S'} p_i p_j (a_i a_j - G(a_i, a_j)) - 2q_2(p_1 + \sum_{i \in S'} a_i p_i)
\end{aligned}$$

(B.7)

With the help of the second inequality in (B.5), and the case $q_2 \geq 0$ under consideration, we deduce that the terms in the second line above are smaller or equal to 0, so that

$$\text{Diff}(p_{\text{gen}}, p_*) \leq -2q_2^2 - 2 \sum_{i \in S'} a_i(a_i - 1)p_i^2 - 2(q_2 + 1) \sum_{i \in S'} (a_i - G(2, a_i))p_i \quad (\text{B.8})$$

Now note that the last two sums are strictly negative for any non-zero p_i , with $i \in \{3, \dots, K\}$. The only way for these to be zero is to set the p_i to zero. And further the only way the first term is zero is $q_2 = 0$. These conditions force $p_{\text{gen}} = p_*$. Therefore for any $p_{\text{gen}} \neq p_*$, $\text{Diff}(p_{\text{gen}}, p_*) < 0$.

If we relax the condition $q_2 \geq 0$ and allow $q_2 = -1$, we can get $\text{Diff}(p_{\text{gen}}, p_*) > 0$ for $p_{\text{gen}} = [1^{p_1}]$ and $p_* = [1^{p_1-2}, 2]$, i.e. $p_3 p_4, \dots, p_K$ all being zero. Indeed setting $q_2 = -1, p_1 = N - 2$ in (B.4) we see that $\text{Diff}(p_{\text{gen}}, p_*) = -2 + 2(N - 2) = 2N - 2$. This recovers recovering the fact in section 5.1 that the most singular term in $\mathcal{Z}(N, x)$ is $\mathcal{Z}(N, p = [1^N], x)$ where the degree exceeds that of $p = [2, 1^{N-2}]$ by $(2N - 2)$.

The only case left is $q_2 = -1$, i.e. $p_2 = 0$, but some of the $p_3, p_4 \dots$ not equal to zero. With these conditions, we want to show that $\text{Diff}(p_{\text{gen}}, p_*) < 0$. Substituting $q_2 = -1$ in (B.7) we have

$$\begin{aligned} \text{Diff}(p_{\text{gen}}, p_*) &= -2 - \sum_{i \in S'} a_i(a_i - 1)p_i^2 - 2p_1 \sum_{i \in S'} p_i(a_i - 1) \\ &\quad - 2 \sum_{i < j \in S'} p_i p_j (a_i a_j - G(a_i, a_j)) + 2p_1 + 2 \sum_{i \in S'} a_i p_i \\ &= -2 - \sum_{i \in S'} (a_i(a_i - 1)p_i^2 - 2a_i p_i) - 2p_1 \left(\sum_{i \in S'} p_i(a_i - 1) - 2 \right) \\ &\quad - 2 \sum_{i < j \in S'} p_i p_j (a_i a_j - G(a_i, a_j)) \end{aligned} \quad (\text{B.9})$$

Consider the term proportional to p_1 . It is useful to recall that $S' = \{3, 4, \dots, K\}$ and $a_K > a_{K-1} > \dots > a_4 > a_3 \geq 3$. If for some $i \in S'$, $p_i > 0$, then $p_i(a_i - 1) \geq 2$ so $-2(p_i(a_i - 1) - 2) < 0$. Also observe that

$$\begin{aligned} - (a_i(a_i - 1)p_i^2 - 2a_i p_i) &= -a_i ((a_i - 1)p_i^2 - 2p_i) \\ &\leq -a_i ((a_i - 1)p_i^2 - 2p_i^2) = -a_i(a_i - 2)p_i^2 \end{aligned} \quad (\text{B.10})$$

Using $(a_i - 2) > 0$ for $i \in S'$, it follows that this is less than 0 for any non-zero p_i . We conclude that the difference of degrees in (B.9).

This completes the proof, that $\text{Diff}(p_{\text{gen}}, p_*) < 0$ for all $p_{\text{gen}} \neq [1^N]$ and $p_{\text{gen}} \neq p_* = [1^N, 2]$. With this result rigorously established for all N , the comparison between the two leading terms in section 5.2 leads to the estimate $x_c \sim \frac{\log N}{N}$ for the breakdown of the high temperature expansion. An interesting problem is to obtain further results for general N on the characteristics of the ordering on partitions given by the degree function (5.5).

C Integer sequences, Hagedorn and heat capacity

We have made use of discrete derivatives in the discussion of the thermodynamics of quantum mechanical degrees of freedom consisting of matrices or tensors in the bulk of the paper. In the systems of interest the stable limit of the degeneracies are integer sequences, several of which are among standard ones tabulated in the OEIS. It is interesting to observe that thermodynamic considerations and associated discrete derivatives give useful perspectives on any sequence of positive integers. The convergence properties, of the sequence itself and of derived sequences related to a given sequence by taking successive ratios, are simply stated in terms of thermodynamic quantities for quantum mechanical systems naturally associated to the sequences.

Given any sequence of positive integers,

$$a_0 = 1, a_1, a_2, a_3, \dots \quad (\text{C.1})$$

We can consider a Hilbert space with a unique vacuum and degeneracies a_n at energies $n \in \{1, 2, \dots\}$. The canonical partition function is

$$Z(x) = \sum_{n=0}^{\infty} a_n x^n \quad (\text{C.2})$$

with $x = e^{-\beta}$. The micro-canonical ensemble degeneracies are $\Omega(n) = a_n$, and the micro-canonical entropy is $S(n) = \log a_n$. The canonical partition function is

$$Z(\beta) = \sum_{n=0}^{\infty} e^{S(n) - \beta n} \quad (\text{C.3})$$

Defining $A_n = a_n e^{-\beta n}$, and using the ratio test, we know that

$$\begin{aligned} \lim_{n \rightarrow \infty} \frac{A_{n+1}}{A_n} < 1 &\text{ implies } Z(\beta) \text{ converges} \\ \lim_{n \rightarrow \infty} \frac{A_{n+1}}{A_n} > 1 &\text{ implies } Z(\beta) \text{ diverges} \end{aligned} \quad (\text{C.4})$$

Expressing in terms of the discrete derivative (4.5)

$$\frac{A_{n+1}}{A_n} = e^{S(n+1) - S(n) - \beta} = e^{DS(n+1) - \beta} \quad (\text{C.5})$$

Sufficient condition for

$$\begin{aligned} \text{Convergence : } \lim_{n \rightarrow \infty} DS(n+1) - \beta &< 0 \\ \text{Divergence: } \lim_{n \rightarrow \infty} DS(n+1) - \beta &> 0 \end{aligned} \quad (\text{C.6})$$

Setting $\beta = 0$, i.e. in the infinite canonical temperature limit, we have the convergence condition of the integer sequence itself. Note these are sufficient conditions but not necessary : if the limit of ratios in (C.4) is 1, then the sequence can be convergent or divergent. This can be stated in terms of the micro-canonical temperature $T_{\text{micro}}(n)$ or inverse temperature $\beta_{\text{micro}}(n) = T_{\text{micro}}^{-1}(n)$. Defining

$$\beta_{\text{micro}}(\infty) = \lim_{n \rightarrow \infty} \beta_{\text{micro}}(n) \quad (\text{C.7})$$

the sufficient conditions are

$$\begin{aligned} \text{Convergence : } & \beta_{\text{micro}}(\infty) - \beta < 0 \\ \text{Divergence: } & \beta_{\text{micro}}(\infty) - \beta > 0 \end{aligned} \quad (\text{C.8})$$

An interesting physical characteristic of the thermodynamics is whether the heat capacity in the micro-canonical ensemble is positive or not. This can be expressed in terms of convergence conditions of the sequence of ratios of successive terms in the sequence $\{a_n\}$.

$$b_1 = a_1, \quad b_2 = \frac{a_2}{a_1}, \quad b_3 = \frac{a_3}{a_2}, \quad b_4 = \frac{a_4}{a_3}, \dots \quad (\text{C.9})$$

Convergence conditions for the sequence $\{b_n\}$ are expressed in terms of the large n behaviour of

$$\frac{b_{n+1}}{b_n} = \frac{a_{n+2}a_n}{a_{n+1}^2} \quad (\text{C.10})$$

The logarithm is

$$\log\left(\frac{a_{n+2}a_n}{a_{n+1}^2}\right) = S(n+2) + S(n) - 2S(n+1) = (D^2S)(n+1) \quad (\text{C.11})$$

The ratio test then gives the sufficient conditions :

$$\begin{aligned} \text{Convergence: } & \lim_{n \rightarrow \infty} D^2S(n+1) < 0 \\ \text{Divergence: } & \lim_{n \rightarrow \infty} D^2S(n+1) > 0 \end{aligned} \quad (\text{C.12})$$

for the derived sequence of successive ratios. Assuming that $\lim_{n \rightarrow \infty} \beta_{\text{micro}}(n)$ is finite and positive, these conditions are expressible in terms of $C_{\text{sh;micro}}(n) = \frac{-\beta_{\text{micro}}^2(n)}{D^2S(n+1)}$. The sufficient conditions are :

$$\begin{aligned} \text{Convergence: } & \lim_{n \rightarrow \infty} C_{\text{hc;micro}}(n) > 0 \\ \text{Divergence: } & \lim_{n \rightarrow \infty} C_{\text{hc;micro}}(n) < 0 \end{aligned} \quad (\text{C.13})$$

By iterating this observation (C.12), we may define the r 'th derived sequence for a given integer sequence by applying r -times the operation of taking successive ratios. The sufficient conditions of convergence for the r 'th derived sequence are expressed in terms of the limit of the $(r + 1)$ 'th derivatives of the entropies of the original sequence.

As an example, the stable sequence for the permutation invariant matrix model has the properties:

$$\lim_{n \rightarrow \infty} DS(n+1) - \beta > 0 \quad \text{for all } \beta \quad (\text{C.14})$$

Thus it has zero Hagedorn temperature. And

$$\lim_{n \rightarrow \infty} D^2S(n+1) > 0 \quad (\text{C.15})$$

Thus the sequence of successive ratios of degeneracies diverges and this corresponds to the negative heat capacity.

D SAGE computation for zero charge sector of 2-matrix models

This uses the `lrcalc` package [87] in SAGE for efficient computation of Littlewood-Richardson coefficients.

```
import sage.libs.lrcalc.lrcalc as lrcalc
def TruncLN ( LRDict , N ) :
    L = list ( LRDict.items() )
    LL = [ L [i] for i in range ( len ( L ) ) if len ( L[i][0] ) < N+1 ]
    return LL
def ListToSumSq ( LRDictList ) :
    L = LRDictList
    SS = 0
    for i in range ( len ( L ) ) :
        SS = SS + (L[i][1])^2
    return SS
def ZZMat0Charge ( n , N ) :
    L1 = len ( Partitions(n).list() )
    S = 0
    P = Partitions(n).list()
    for i in range(L1):
        for j in range(L1):
            if len( Partitions(n).list()[i] ) < N+1 :
                if len( Partitions(n).list()[j] ) < N+1 :
                    S = S + ListToSumSq ( TruncLN ( lrcalc.mult ( Partitions(n).list()[i] , Partitions(n).list()[j] ) , N ) )
    return S
```

E SAGE computation for negative SHC in multi-matrix model with $d = n$ scaling

First we set up the basic objects :

```
# Setting up Schur symmetric functions and power sum symmetric functions in SAGE ; and formulae for Dimension of the U(d)
# representation associated with Young diagram p having n boxes
s = SymmetricFunctions(QQ).s()
pp = SymmetricFunctions(QQ).power()
var ("d")
def DimmGenNum ( d , p , n ) :
    return prod ( prod ( ( d - i + k ) for k in range (p[i] ) ) for i in range ( len ( p )))
def DimmGen ( d , p , n ) :
    return DimmGenNum ( d , p , n )*dimension(p)/factorial (n)
```

Then the computation of the state degeneracies follows:

```
## Counting states at energy n in d-matrix harmonic oscillator where d is set to n, using character sum
# (simpler than summing over Kronecker coefficients )
def Zmultmatdegn ( n , N ) :
    L = len ( Partitions(n).list() )
    S = 0
    P = Partitions(n).list()
    for i in range(L):
        for j in range(L):
            if len( Partitions(n).list()[i]) < N+1 :
                S = S + (s(P[i]).scalar(pp(P[j])))**2/P[j].centralizer_size()*n**(len (P[j]))
    return S
```

References

- [1] T. Banks, W. Fischler, S. H. Shenker and L. Susskind, “M theory as a matrix model: A Conjecture,” *Phys. Rev. D* **55** (1997), 5112-5128 doi:10.1103/PhysRevD.55.5112 [arXiv:hep-th/9610043 [hep-th]].
- [2] D. E. Berenstein, J. M. Maldacena and H. S. Nastase, “Strings in flat space and pp waves from N=4 superYang-Mills,” *JHEP* **04** (2002), 013 doi:10.1088/1126-6708/2002/04/013 [arXiv:hep-th/0202021 [hep-th]].
- [3] J. M. Maldacena, “The Large N limit of superconformal field theories and supergravity,” *Adv. Theor. Math. Phys.* **2** (1998), 231-252 doi:10.4310/ATMP.1998.v2.n2.a1 [arXiv:hep-th/9711200 [hep-th]].
- [4] E. Witten, “Anti-de Sitter space and holography,” *Adv. Theor. Math. Phys.* **2** (1998), 253-291 doi:10.4310/ATMP.1998.v2.n2.a2 [arXiv:hep-th/9802150 [hep-th]].
- [5] S. S. Gubser, I. R. Klebanov and A. M. Polyakov, “Gauge theory correlators from noncritical string theory,” *Phys. Lett. B* **428** (1998), 105-114 doi:10.1016/S0370-2693(98)00377-3 [arXiv:hep-th/9802109 [hep-th]].
- [6] D. O’Connor and S. Ramgoolam, “Gauged permutation invariant matrix quantum mechanics: path integrals,” *JHEP* **04** (2024), 080 doi:10.1007/JHEP04(2024)080 [arXiv:2312.12397 [hep-th]].
- [7] D. O’Connor and S. Ramgoolam, “Gauged permutation invariant matrix quantum mechanics: Partition functions,” [arXiv:2312.12398 [hep-th]].
- [8] O. Aharony, J. Marsano, S. Minwalla, K. Papadodimas and M. Van Raamsdonk, “The Hagedorn - deconfinement phase transition in weakly coupled large N gauge theories,” *Adv. Theor. Math. Phys.* **8** (2004), 603-696 doi:10.4310/ATMP.2004.v8.n4.a1 [arXiv:hep-th/0310285 [hep-th]].
- [9] B. Sundborg, “The Hagedorn transition, deconfinement and N=4 SYM theory,” *Nucl. Phys. B* **573** (2000), 349-363 doi:10.1016/S0550-3213(00)00044-4 [arXiv:hep-th/9908001 [hep-th]].

- [10] A. T. Kristensson and M. Wilhelm, “From Hagedorn to Lee-Yang: partition functions of $\mathcal{N} = 4$ SYM theory at finite N ,” JHEP **10** (2020), 006 doi:10.1007/JHEP10(2020)006 [arXiv:2005.06480 [hep-th]].
- [11] Y. Asano, V. G. Filev, S. Kováčik and D. O’Connor, “The non-perturbative phase diagram of the BMN matrix model,” JHEP **07** (2018), 152 doi:10.1007/JHEP07(2018)152 [arXiv:1805.05314 [hep-th]].
- [12] S. Kováčik, D. O’Connor and Y. Asano, “The nonperturbative phase diagram of the bosonic BMN matrix model,” PoS **CORFU2019** (2020), 221 doi:10.22323/1.376.0221 [arXiv:2004.05820 [hep-th]].
- [13] V. G. Filev and D. O’Connor, “The BFSS model on the lattice,” JHEP **05** (2016), 167 doi:10.1007/JHEP05(2016)167 [arXiv:1506.01366 [hep-th]].
- [14] D. J. Gross and W. Taylor, “Two-dimensional QCD is a string theory,” Nucl. Phys. B **400** (1993), 181-208 doi:10.1016/0550-3213(93)90403-C [arXiv:hep-th/9301068 [hep-th]].
- [15] J. A. Minahan and A. P. Polychronakos, “Equivalence of two-dimensional QCD and the $C = 1$ matrix model,” Phys. Lett. B **312** (1993), 155-165 doi:10.1016/0370-2693(93)90504-B [arXiv:hep-th/9303153 [hep-th]].
- [16] S. Corley, A. Jevicki and S. Ramgoolam, “Exact correlators of giant gravitons from dual $N=4$ SYM theory,” Adv. Theor. Math. Phys. **5** (2002), 809-839 [arXiv:hep-th/0111222 [hep-th]].
- [17] D. Berenstein, “A Toy model for the AdS / CFT correspondence,” JHEP **07** (2004), 018 doi:10.1088/1126-6708/2004/07/018 [arXiv:hep-th/0403110 [hep-th]].
- [18] Y. Takayama and A. Tsuchiya, “Complex matrix model and fermion phase space for bubbling AdS geometries,” JHEP **10** (2005), 004 doi:10.1088/1126-6708/2005/10/004 [arXiv:hep-th/0507070 [hep-th]].
- [19] Y. Kimura, S. Ramgoolam and D. Turton, “Free particles from Brauer algebras in complex matrix models,” JHEP **05** (2010), 052 doi:10.1007/JHEP05(2010)052 [arXiv:0911.4408 [hep-th]].
- [20] T. Harmark and M. Orselli, “Spin Matrix Theory: A quantum mechanical model of the AdS/CFT correspondence,” JHEP **11** (2014), 134 doi:10.1007/JHEP11(2014)134 [arXiv:1409.4417 [hep-th]].
- [21] S. Cordes, G. W. Moore and S. Ramgoolam, “Lectures on 2-d Yang-Mills theory, equivariant cohomology and topological field theories,” Nucl. Phys. B Proc. Suppl. **41** (1995), 184-244 doi:10.1016/0920-5632(95)00434-B [arXiv:hep-th/9411210 [hep-th]].

- [22] S. Ramgoolam, “Schur-Weyl duality as an instrument of Gauge-String duality,” AIP Conf. Proc. **1031** (2008) no.1, 255-265 doi:10.1063/1.2972012 [arXiv:0804.2764 [hep-th]].
- [23] N. Ishibashi, H. Kawai, Y. Kitazawa and A. Tsuchiya, “A Large N reduced model as superstring,” Nucl. Phys. B **498** (1997), 467-491 doi:10.1016/S0550-3213(97)00290-3 [arXiv:hep-th/9612115 [hep-th]].
- [24] E. Wigner, “Random Matrices in Physics,” SIAM Reviews v.9 (1967) No. 1, 1-23
- [25] T. Guhr, A. Muller-Groeling, and H.A. Weidenmuller, “Random-matrix theories in quantum physics: common concepts,” Physics Reports, 299(4):189-425, 1998.
- [26] A. Edelman and Y. Wang. Random matrix theory and its innovative applications. In Advances in Applied Mathematics, Modeling, and Computational Science, pages 91-116. Springer, 2013.
- [27] D. Kartsaklis, S. Ramgoolam and M. Sadrzadeh, “Linguistic matrix theory,” Ann. Inst. H. Poincare D Comb. Phys. Interact. **6** (2019) no.3, 385-426 doi:10.4171/aihpd/75 [arXiv:1703.10252 [cs.CL]].
- [28] S. Ramgoolam, “Permutation invariant Gaussian matrix models,” Nucl. Phys. B **945** (2019), 114682 doi:10.1016/j.nuclphysb.2019.114682 [arXiv:1809. [hep-th]].
- [29] S. Ramgoolam, M. Sadrzadeh and L. Sword, “Gaussianity and typicality in matrix distributional semantics,” Ann. Inst. H. Poincare D Comb. Phys. Interact. **9** (2022) no.1, 1-45 doi:10.4171/aihpd/112 [arXiv:1912.10839 [hep-th]].
- [30] M. A. Huber, A. Correia, S. Ramgoolam and M. Sadrzadeh, “Permutation invariant matrix statistics and computational language tasks,” [arXiv:2202.06829 [cs.CL]].
- [31] G. Barnes, S. Ramgoolam and M. Stephanou, “Permutation invariant Gaussian matrix models for financial correlation matrices,” [arXiv:2306.04569 [q-fin.ST]].
- [32] G. Barnes, A. Padellaro and S. Ramgoolam, “Hidden symmetries and large N factorisation for permutation invariant matrix observables,” JHEP **08** (2022), 090 doi:10.1007/JHEP08(2022)090 [arXiv:2112.00498 [hep-th]].
- [33] G. Barnes, A. Padellaro and S. Ramgoolam, “Permutation symmetry in large-N matrix quantum mechanics and partition algebras,” Phys. Rev. D **106** (2022) no.10, 106020 doi:10.1103/PhysRevD.106.106020 [arXiv:2207.02166 [hep-th]].
- [34] G. Barnes, A. Padellaro and S. Ramgoolam, “Permutation invariant Gaussian two-matrix models,” J. Phys. A **55** (2022) no.14, 145202 doi:10.1088/1751-8121/ac4de1 [arXiv:2104.03707 [hep-th]].

- [35] OEIS Foundation Inc. (2024), The On-Line Encyclopedia of Integer Sequences, <https://oeis.org/A052171>
- [36] R. Gurau, “The $1/N$ expansion of colored tensor models,” *Annales Henri Poincaré* **12** (2011), 829-847 doi:10.1007/s00023-011-0101-8 [arXiv:1011.2726 [gr-qc]].
- [37] R. Gurau and V. Rivasseau, The $1=N$ expansion of colored tensor models in arbitrary dimension. *Europhys. Lett.* 95 (2011), Article Id. 50004.
- [38] J. Ben Geloun and S. Ramgoolam, “Counting tensor model observables and branched covers of the 2-sphere,” *Ann. Inst. H. Poincaré D Comb. Phys. Interact.* **1** (2014) no.1, 77-138 doi:10.4171/aihpd/4 [arXiv:1307.6490 [hep-th]].
- [39] J. Ben Geloun and S. Ramgoolam, “All-orders asymptotics of tensor model observables from symmetries of restricted partitions,” *J. Phys. A* **55** (2022) no.43, 435203 doi:10.1088/1751-8121/ac9b3b [arXiv:2106.01470 [hep-th]].
- [40] OEIS Foundation Inc. (2024), The On-Line Encyclopedia of Integer Sequences, <https://oeis.org/A110143>
- [41] K. Bulycheva, I. R. Klebanov, A. Milekhin and G. Tarnopolsky, “Spectra of Operators in Large N Tensor Models,” *Phys. Rev. D* **97** (2018) no.2, 026016 doi:10.1103/PhysRevD.97.026016 [arXiv:1707.09347 [hep-th]].
- [42] M. Beccaria and A. A. Tseytlin, “Partition function of free conformal fields in 3-plet representation,” *JHEP* **05** (2017), 053 doi:10.1007/JHEP05(2017)053 [arXiv:1703.04460 [hep-th]].
- [43] V. Drensky, *Computing with Matrix Invariants*, Mathematica Balkanica, New Series Vol. 21, 2007, Fasc. 1-2
- [44] H. Touchette, “Equivalence and Nonequivalence of Ensembles: Thermodynamic, Macrostate, and Measure Levels.” *J Stat Phys* (2015) 159:987–1016
- [45] B. Bollobas, “The asymptotic number of unlabelled regular graphs,” *J. London Math. Soc.* (2), 26 (1982), 201-206
- [46] Dragomir Ž. Đoković, Poincaré series of some pure and mixed trace algebras of two generic matrices, *Journal of Algebra* **309** (2007) 654–671; arXiv:math/0609262 [math.AC]
- [47] Murty S. S. Challa, D. P. Landau, and K. Binder “Finite-size effects at temperature-driven first-order transitions,” *Phys. Rev. B* 34, 1841 – Published 1 August 1986
- [48] D. Berenstein, “Submatrix deconfinement and small black holes in AdS,” *JHEP* **09** (2018), 054 doi:10.1007/JHEP09(2018)054 [arXiv:1806.05729 [hep-th]].

- [49] Denjoe O’ Connor, Talk at ESI workshop on Large N matrix models and Emergent Geometry, 04/09/23-09/09/23; <https://www.esi.ac.at/events/t1307/>; paper to appear.
- [50] F. A. Dolan, “Counting BPS operators in N=4 SYM,” Nucl. Phys. B **790** (2008), 432-464 doi:10.1016/j.nuclphysb.2007.07.026 [arXiv:0704.1038 [hep-th]].
- [51] M. Bianchi, F. A. Dolan, P. J. Heslop and H. Osborn, “N=4 superconformal characters and partition functions,” Nucl. Phys. B **767** (2007), 163-226 doi:10.1016/j.nuclphysb.2006.12.005 [arXiv:hep-th/0609179 [hep-th]].
- [52] S. Ramgoolam, M. C. Wilson and A. Zahabi, “Quiver Asymptotics: $\mathcal{N} = 1$ Free Chiral Ring,” J. Phys. A **53** (2020) no.10, 105401 [arXiv:1811.11229 [hep-th]].
- [53] M. Hanada and J. Maltz, “A proposal of the gauge theory description of the small Schwarzschild black hole in $\text{AdS}_5 \times \text{S}^5$,” JHEP **02** (2017), 012 doi:10.1007/JHEP02(2017)012 [arXiv:1608.03276 [hep-th]].
- [54] D. Berenstein, “Submatrix deconfinement and small black holes in AdS,” JHEP **09** (2018), 054 doi:10.1007/JHEP09(2018)054 [arXiv:1806.05729 [hep-th]].
- [55] Y. Takayama and A. Tsuchiya, “Complex matrix model and fermion phase space for bubbling AdS geometries,” JHEP **10** (2005), 004 doi:10.1088/1126-6708/2005/10/004 [arXiv:hep-th/0507070 [hep-th]].
- [56] H. Lin, O. Lunin and J. M. Maldacena, JHEP **10** (2004), 025 doi:10.1088/1126-6708/2004/10/025 [arXiv:hep-th/0409174 [hep-th]].
- [57] A. Dhar, G. Mandal and N. V. Suryanarayana, “Exact operator bosonization of finite number of fermions in one space dimension,” JHEP **01** (2006), 118 doi:10.1088/1126-6708/2006/01/118 [arXiv:hep-th/0509164 [hep-th]].
- [58] V. Balasubramanian, J. de Boer, V. Jejjala and J. Simon, “The Library of Babel: On the origin of gravitational thermodynamics,” JHEP **12** (2005), 006 doi:10.1088/1126-6708/2005/12/006 [arXiv:hep-th/0508023 [hep-th]].
- [59] V. Balasubramanian, B. Czech, K. Larjo and J. Simon, “Integrability versus information loss: A Simple example,” JHEP **11** (2006), 001 doi:10.1088/1126-6708/2006/11/001 [arXiv:hep-th/0602263 [hep-th]].
- [60] R. Gurau, “Random tensors,” Oxford University Press, 2016.
- [61] M. Ouerfelli, V. Rivasseau and M. Tamaazousti, “The Tensor Track VII: From Quantum Gravity to Artificial Intelligence,” [arXiv:2205.10326 [hep-th]].
- [62] P. Diaz and S. J. Rey, “Orthogonal Bases of Invariants in Tensor Models,” JHEP **02** (2018), 089 doi:10.1007/JHEP02(2018)089 [arXiv:1706.02667 [hep-th]].

- [63] R. de Mello Koch, D. Gossman and L. Tribelhorn, “Gauge Invariants, Correlators and Holography in Bosonic and Fermionic Tensor Models,” *JHEP* **09** (2017), 011 doi:10.1007/JHEP09(2017)011 [arXiv:1707.01455 [hep-th]].
- [64] J. Ben Geloun and S. Ramgoolam, “Tensor Models, Kronecker coefficients and Permutation Centralizer Algebras,” *JHEP* **11** (2017), 092 doi:10.1007/JHEP11(2017)092 [arXiv:1708.03524 [hep-th]].
- [65] <https://www.sagemath.org/>
- [66] <https://doc.sagemath.org/html/en/reference/combinat/sage/combinat/sf/schur.html>
- [67] S. W. Hawking and D. N. Page, “Thermodynamics of Black Holes in anti-De Sitter Space,” *Commun. Math. Phys.* **87** (1983), 577 doi:10.1007/BF01208266
- [68] R. Pemantle and M.C. Wilson (2013) “Analytic Combinatorics in Several Variables,” Cambridge University Press (Cambridge Studies in Advanced Mathematics), pp. i–vi.
- [69] Y. Kimura and S. Ramgoolam, “Branes, anti-branes and brauer algebras in gauge-gravity duality,” *JHEP* **11** (2007), 078 [arXiv:0709.2158 [hep-th]].
- [70] W. Thirring, “Systems with Negative Specific Heat,” *Z. Physik* **235**, 339-352 (1970)
- [71] Alessandro Campaa, Thierry Dauxois, Stefano Ruffo, “Statistical mechanics and dynamics of solvable models with long-range interactions,” *Physics Reports* **480** (2009) 57-159
- [72] R. Bhattacharyya, S. Collins and R. de Mello Koch, “Exact Multi-Matrix Correlators,” *JHEP* **03** (2008), 044 doi:10.1088/1126-6708/2008/03/044 [arXiv:0801.2061 [hep-th]].
- [73] R. Bhattacharyya, R. de Mello Koch and M. Stephanou, “Exact Multi-Restricted Schur Polynomial Correlators,” *JHEP* **06** (2008), 101 doi:10.1088/1126-6708/2008/06/101 [arXiv:0805.3025 [hep-th]].
- [74] T. W. Brown, P. J. Heslop and S. Ramgoolam, “Diagonal multi-matrix correlators and BPS operators in N=4 SYM,” *JHEP* **02** (2008), 030 doi:10.1088/1126-6708/2008/02/030 [arXiv:0711.0176 [hep-th]].
- [75] T. W. Brown, P. J. Heslop and S. Ramgoolam, “Diagonal free field matrix correlators, global symmetries and giant gravitons,” *JHEP* **04** (2009), 089 doi:10.1088/1126-6708/2009/04/089 [arXiv:0806.1911 [hep-th]].
- [76] S. Collins, “Restricted Schur Polynomials and Finite N Counting,” *Phys. Rev. D* **79** (2009), 026002 doi:10.1103/PhysRevD.79.026002 [arXiv:0810.4217 [hep-th]].

- [77] S. Murthy, “Unitary matrix models, free fermions, and the giant graviton expansion,” *Pure Appl. Math. Quart.* **19** (2023) no.1, 299-340 doi:10.4310/PAMQ.2023.v19.n1.a12 [arXiv:2202.06897 [hep-th]].
- [78] C. T. Asplund and D. Berenstein, “Small AdS black holes from SYM,” *Phys. Lett. B* **673** (2009), 264-267 doi:10.1016/j.physletb.2009.02.043 [arXiv:0809.0712 [hep-th]].
- [79] F. Ferrari, “The large D limit of planar diagrams,” *Ann. Inst. H. Poincaré D Comb. Phys. Interact.* **6** (2019) no.3, 427-448 doi:10.4171/aihpd/76 [arXiv:1701.01171 [hep-th]].
- [80] I. R. Klebanov, F. Popov and G. Tarnopolsky, “TASI Lectures on Large N Tensor Models,” *PoS TASI2017* (2018), 004 doi:10.22323/1.305.0004 [arXiv:1808.09434 [hep-th]].
- [81] R. C. Avouh, J. Ben Geloun and R. Toriumi, “Counting $U(N)^{\otimes r} \otimes O(N)^{\otimes q}$ invariants and tensor model observables,” [arXiv:2404.16404 [hep-th]].
- [82] D. Berenstein, “Negative specific heat from non-planar interactions and small black holes in AdS/CFT,” *JHEP* **10** (2019), 001 doi:10.1007/JHEP10(2019)001 [arXiv:1810.07267 [hep-th]].
- [83] OEIS Foundation Inc. (2024), The On-Line Encyclopedia of Integer Sequences, <https://oeis.org/A279819>
- [84] C. Rebbi, “Monte Carlo Computations for Lattice Gauge Theories with Finite Gauge Groups,” *NATO Sci. Ser. B* **70** (1981), 241-262
- [85] G. Bhanot and C. Rebbi, “Monte Carlo Simulations of Lattice Models With Finite Subgroups of $SU(3)$ as Gauge Groups,” *Phys. Rev. D* **24** (1981), 3319
- [86] P. Hasenfratz and F. Niedermayer, “Unexpected results in asymptotically free quantum field theories,” *Nucl. Phys. B* **596** (2001), 481-494 [arXiv:hep-lat/0006021 [hep-lat]].
- [87] lrcalc package by A. Buch: <https://sites.math.rutgers.edu/~asbuch/lrcalc/>